NTIA-REPORT-80-33

HF Radio Noise in the Topside Ionosphere

C.M. Rush

R.K. Rosich

C. Mellecker

U.S. DEPARTMENT OF COMMERCE
Philip M. Klutznick, Secretary

Henry Geller, Assistant Secretary
for Communications and Information

February 1980

TABLE OF CONTENTS

	Page
LIST OF FIGURES	iv
LIST OF TABLES	viii
ABSTRACT	1
1. INTRODUCTION	1
2. HF RADIO SOURCES ON THE EARTH	2
3. DMSP HF RADIO NOISE CHARACTERISTICS	5
4. DATA ANALYSIS METHODS	7
5. RESULTS OF THE DATA ANALYSIS	8
5.1. Time Interval Averaging	8
5.2. Global Maps of HF Radio Noise	9
5.3. Frequency Dependence of HF Radio Noise	12
5.4. Studies of a Localized Effect	33
5.5. Studies of Seasonal Effects	33
6. COMPARISON OF DATA WITH HF ALLOCATIONS	41
7. CONCLUSION	47
8. REFERENCES	49

LIST OF FIGURES

		Page
Figure 1.	Values of take-off angle (κ) as a function of f_c/f_{ob}	4
Figure 2.	Signal strength (in volts) as a function of frequency observed by the DMSP satellite at 40.4°N, 265.8°E on July 27, 1977	6
Figure 3.	Global distribution of radio noise observed at 12 MHz during the dawn period of September-November 1977. Contours are receiver output voltage (millivolts $\times 10^{-2}$).	11
Figure 4a.	Global distribution of radio noise observed at 11.8 MHz during the dawn period of November 1977. Contours are receiver output voltage (millivolts $\times 10^{-3}$).	13
Figure 4b.	Global distribution of radio noise observed at 11.8 MHz during the dusk period of November 1977. Contours are receiver output voltage (millivolts $\times 10^{-3}$).	14
Figure 5a.	Global distribution of radio noise observed at 9.6 MHz during the dawn period of November 1977. Contours are receiver output voltage (millivolts $\times 10^{-3}$).	15
Figure 5b.	Global distribution of radio noise observed at 9.6 MHz during the dusk period of November 1977. Contours are receiver output voltage (millivolts $\times 10^{-3}$).	16
Figure 6a.	Global distribution of radio noise observed at 6.1 MHz during the dawn period of November 1977. Contours are receiver output voltage (millivolts $\times 10^{-3}$).	17
Figure 6b.	Global distribution of radio noise observed at 6.1 MHz during the dusk period of November 1977. Contours are receiver output voltage (millivolts $\times 10^{-3}$).	18
Figure 7a.	Global distribution of radio noise observed at 8.5 MHz during the dawn period of November 1977. Contours are receiver output voltage (millivolts $\times 10^{-3}$).	19
Figure 7b.	Global distribution of radio noise observed at 8.5 MHz during the dusk period of November 1977. Contours are receiver output voltage (millivolts $\times 10^{-3}$).	20

Figure 8a. Global distribution of radio noise observed at 12.5 MHz during the dawn period of November 1977. Contours are receiver output voltage (millivolts $\times 10^{-3}$). 21

Figure 8b. Global distribution of radio noise observed at 12.5 MHz during the dusk period of November 1977. Contours are receiver output voltage (millivolts $\times 10^{-3}$). 22

Figure 9. Behavior of the HF radio environment at local dawn above Eurasia, North America, and Australia for frequencies of 4.0, 4.5, 5.0 and 5.5 MHz during the period September-November 1977. Contours are receiver output voltage (millivolts $\times 10^{-2}$). 23

Figure 10. Behavior of the HF radio environment at local dawn above Eurasia, North America, and Australia for frequencies of 6.0, 6.5, 7.0, and 7.5 MHz during the period September-November 1977. Contours are receiver output voltage (millivolts $\times 10^{-2}$). 24

Figure 11. Behavior of the HF radio environment at local dawn above Eurasia, North America, and Australia for frequencies of 8.0, 8.5, 9.0, and 9.5 MHz during the period September -November 1977. Contours are receiver output voltage (millivolts $\times 10^{-2}$). 25

Figure 12. Behavior of the HF radio environment at local dawn above Eurasia, North America, and Australia for frequencies of 10.0, 10.5, 11.0, 11.5 MHz during the period September-November 1977. Contours are receiver output voltage (millivolts $\times 10^{-2}$). 26

Figure 13. Behavior of the HF radio environment at local dawn above Eurasia, North America, and Australia for frequencies of 12.0, 12.5, 13.0, 13.5 MHz during the period September-November 1977. Contours are receiver output voltage (millivolts $\times 10^{-2}$). 27

Figure 14. Behavior of the HF radio environment at local dusk above Eurasia, North America, and Australia for frequencies of 4.0, 4.5, 5.0 and 5.5 MHz during the period September-November 1977. Contours are receiver output voltage (millivolts $\times 10^{-2}$). 28

Figure 15. Behavior of the HF radio environment at local dusk above Eurasia, North America, and Australia for frequencies of 6.0. 6.5, 7.0, and 7.5 MHz during the period September-November 1977. Contours are receiver output voltage (millivolts $\times 10^{-2}$). 29

Figure 16. Behavior of the HF radio environment at local dusk above Eurasia, North America, and Australia for frequencies of 8.0, 8.5, 9.0, and 9.5 MHz during the period September-November 1977. Contours are receiver output voltage (millivolts $\times 10^{-2}$). 30

Figure 17. Behavior of the HF radio environment at local dusk above Eurasia, North America, and Australia for frequencies of 10.0, 10.5, 11.0, 11.5 MHz during the period September-November 1977. Contours are receiver output voltage (millivolts $\times 10^{-2}$). 31

Figure 18. Behavior of the HF radio environment at local dusk above Eurasia, North America, and Australia for frequencies 12.0, 12.5, 13.0, 13.5 MHz during the period September-November 1977. Contours are receiver output voltage (millivolts $\times 10^{-2}$). 32

Figure 19. Contours of the receiver output voltage observed at 11.5 MHz during the times indicated. Contours are given in millivolts $\times 10^{-3}$ 34

Figure 20a. Global distribution of radio noise observed at 11.8 MHz during the dawn period of April 1978 Contours are receiver output voltage (millivolts $\times 10^{-3}$). 35

Figure 20b. Global distribution of radio noise observed at 11.8 Mhz during the dusk period of April 1978. Contours are receiver output voltage (millivolts $\times 10^{-3}$). 36

Figure 21a. Global distribution of radio noise observed at 8.5 MHz during the dawn period of April 1978. Contours are receiver output voltage (millivolts $\times 10^{-3}$). 37

Figure 21b. Global distribution of radio noise observed at 8.5 MHz during the dusk period of April 1978. Contours are receiver output voltage (millivolts $\times 10^{-3}$). 38

Figure 22a. Global distribution of radio noise observed at 12.5 MHz during the dawn period of April 1978 Contours are receiver output voltage (millivolts $\times 10^{-3}$). 39

Figure 22b. Global distribution of radio noise observed at 12.5 MHz during the dusk period of April 1978. Contours are receiver output voltage (millivolts $\times 10^{-3}$). 40

Figure 23. Global distribution of radio noise observed at 11.3 MHz during the dawn period of November 1977 averaged over 100 KHz. Contours are given in receiver output voltage (millivolts × 10^{-3}). 45

Figure 24. Global distribution of radio noise observed at 11.3 MHz during the dawn period of November 1977 averaged over 1.2 MHz. Contours are given in receiver output voltage (millivolts × 10^{-3}). 46

LIST OF TABLES

		Page
Table 1.	Values of HF Receiver Counts for 8.5 and 11.7 MHz Averaged Over 5, 10, and 15 Day Intervals.	10
Table 2.	Classes of Radio Services Allocated within ±100 KHz of the Frequency Indicated.	43

HF RADIO NOISE IN THE TOPSIDE IONOSPHERE

Charles M. Rush, Rayner K. Rosich, and Carlene Mellecker*

Radio noise of ground-based origin can be observed by a satellite-borne receiver orbiting above the F2 region. The noise that is observed is a function of receiver frequency, satellite position, and local time at the sub-satellite point. A recently launched Defense Meteorological Satellite is equipped with a swept-frequency, high-frequency (HF) noise receiver and currently is providing data on a routine basis all along the satellite orbit. The receiver provides measurements of radio noise of terrestrial origin every 100 kHz in the frequency range 1.2 to 13.9 MHz. In this report, we discuss the characteristics of the noise environment as observed by the satellite during periods surrounding local dawn and local dusk.

KEY WORDS: DMSP Satellite; HF Propagation; HF Radio Noise; Spectrum Utilization.

1. INTRODUCTION

Radio noise measurements have been made at numerous ground-based locations for many years. These measurements were undertaken partly because noise can be a limiting factor in the performance of radio communication systems. Ground-based measurements obviously are confined to regions determined by political and geographical considerations. With the advent of satellites, measurements of radio noise could be made within the ionosphere at all locations along the satellite orbit.

Most of the measurements that have been made of radio noise at satellite heights have tended to deal with the noise spectrum associated with galactic, cosmic, and solar sources (Walsh et al., 1964; Hartz, 1964a, 1964b, 1969; Alexander et al., 1969a, 1969b; Hakura et al., 1970). Noise of magnetospheric origin has also been observed and related to auroral activity (Kurth et al., 1975; Gurnett, 1975). A few studies (for example, Horner and Bent, 1969; Herman et al., 1973) have been devoted to detailing the HF noise environment at satellite heights. Further studies by Herman et al. (1975) attempted to relate satellite HF noise observations to terrestrial thunderstorm sources. More recently, measurements have been made using the atmospheric radio-noise experiment operating on-board the Japanese satellite, ISS-B (Wakai, 1978, private communication). It is anticipated that these measurements will yield information that will result in an improved representation of the noise environment at satellite heights due to terrestrial lightning sources. Such

*The authors are with the U.S. Department of Commerce, National Telecommunications and Information Administration, Institute for Telecommunication Sciences, Boulder, Colorado 80303.

information would prove extremely useful in improving the maps of atmospheric noise given by the International Radio Consultative Committee (CCIR) in Report 322 (CCIR, 1963), assuming that the noise received at the satellite could be directly compared to the noise received at the surface of the earth.

Electromagnetic waves, be they "noise" or distinct signals, when propagated from the earth's surface to orbiting satellites, are influenced by the ionosphere. The ionosphere behaves essentially as a high-pass filter with respect to radio energy propagated through it from the earth's surface. The low-frequency cut-off of this filter corresponds to foF2, the F2 region critical frequency. Utilizing the characteristics of this ionospheric high pass-filter, Rush and Buchau (1977) were able to discuss the feasibility of deducing the sub-satellite value of foF2 by using HF noise measurements obtained from satellites orbiting above the F2 region. The usefulness of such measurements in determining foF2 under operational conditions has been addressed further by Rush and Ziemba (1978).

In the late Spring of 1977, a satellite in the Air Force Defense Meteorological Satellite Program (DMSP) was launched that was equipped with an HF radio noise receiver to provide measurements of the HF noise environment at the satellite height. Assuming that the noise reaching the satellite emanates from sources on the surface of the earth, investigations were initiated to assess the accuracy of foF2 determined from such data (Rush et al., 1978). In this report, we discuss the results of studies undertaken in order to develop a morphological picture of the radio environment in the ionosphere above the peak of the F2 region. Prior to presenting the results of this effort, we discuss the factors and assumptions that must be considered in assessing the propagation of terrestrially-based signals through the ionosphere to satellite heights. Also, it will prove useful to describe some general characteristics of the DMSP HF receiver before discussing the experimental results.

2. HF RADIO SOURCES ON THE EARTH

Before presenting the results of our study, it is useful to consider the properties of an HF radio signal that originates on the ground and is received at a satellite orbiting above the F2-region peak. In the ensuing discussion, our attention is confined to frequencies greater than $2f_HF2$ where f_HF2 is the electron gyrofrequency at the F2-peak. For the sake of simplicity, it is assumed that a curved ionosphere surrounds a curved earth and that the only variation in the electron density distribution is with altitude, and this variation can be adequately represented by a single parabolic profile. Under these conditions, Snell's Law can be cast into the form:

$$\upsilon\rho \sin \phi = R_E \cos \kappa \tag{1}$$

where υ = the real part of index of refraction at height h,

$\rho = R_E + h$,

R_E = radius of the Earth,

h = height of satellite

ϕ = the angle of incidence of the radio wave at ρ, and

κ = the take-off angle of the radio wave at the surface of the earth.

It can be shown (Maliphant, 1967) that, if the effects of the earth's magnetic field and collisions between particle constituents are unimportant in the determination of the refractive index, an HF wave that penetrates the ionosphere will be governed by

$$\cos \kappa = \frac{hmF2 = R_E}{R_E} \left[1 - \left(\frac{f_c}{f_{ob}} \right)^2 \right]^{1/2} \tag{2}$$

where hmF2 = the height of the F2-region,

f_c = the critical frequency of the F2=region, and

f_{ob} = the frequency of the radio wave.

From equation (2), it follows that, if f_c/f_{ob} is greater than unity, the radio wave is reflected within the ionosphere and is returned to the ground. As f_c/f_{ob} goes from 1 to 0, the radio wave will penetrate the ionosphere at lower and lower take-off angles, assuming f_c is constant over the entire ionosphere.

Figure 1 shows the values of κ as a function of f_c/f_{ob} for heights of the F2-region between 200 and 400 km. It is readily seen that, for values of f_c/f_{ob} slightly less than unity, the value of κ is near 90°. When viewed from the satellite, radio energy penetrating through a homogeneous ionosphere near the critical frequency will emanate from a region on the earth's surface in the immediate vicinity below the satellite height; e.g., the satellite "iris" would approach zero. Frequencies greater than the critical frequency will penetrate through the ionosphere at lower ground take-off angles, which, when viewed from the satellite, implies penetrating through the ionosphere at distances that are correspondingly removed from the sub-satellite point.

The propagation of HF signals from the ground to an orbiting satellite is complicated by the fact that the ionosphere is not horizontally homogeneous. Large gradients in foF2 are typical of the nighttime polar ionosphere, the equatorial ionosphere, and the ionosphere during sunrise and sunset conditions. Thus, it is readily apparent that satellite observations of HF radio noise must be interpreted with

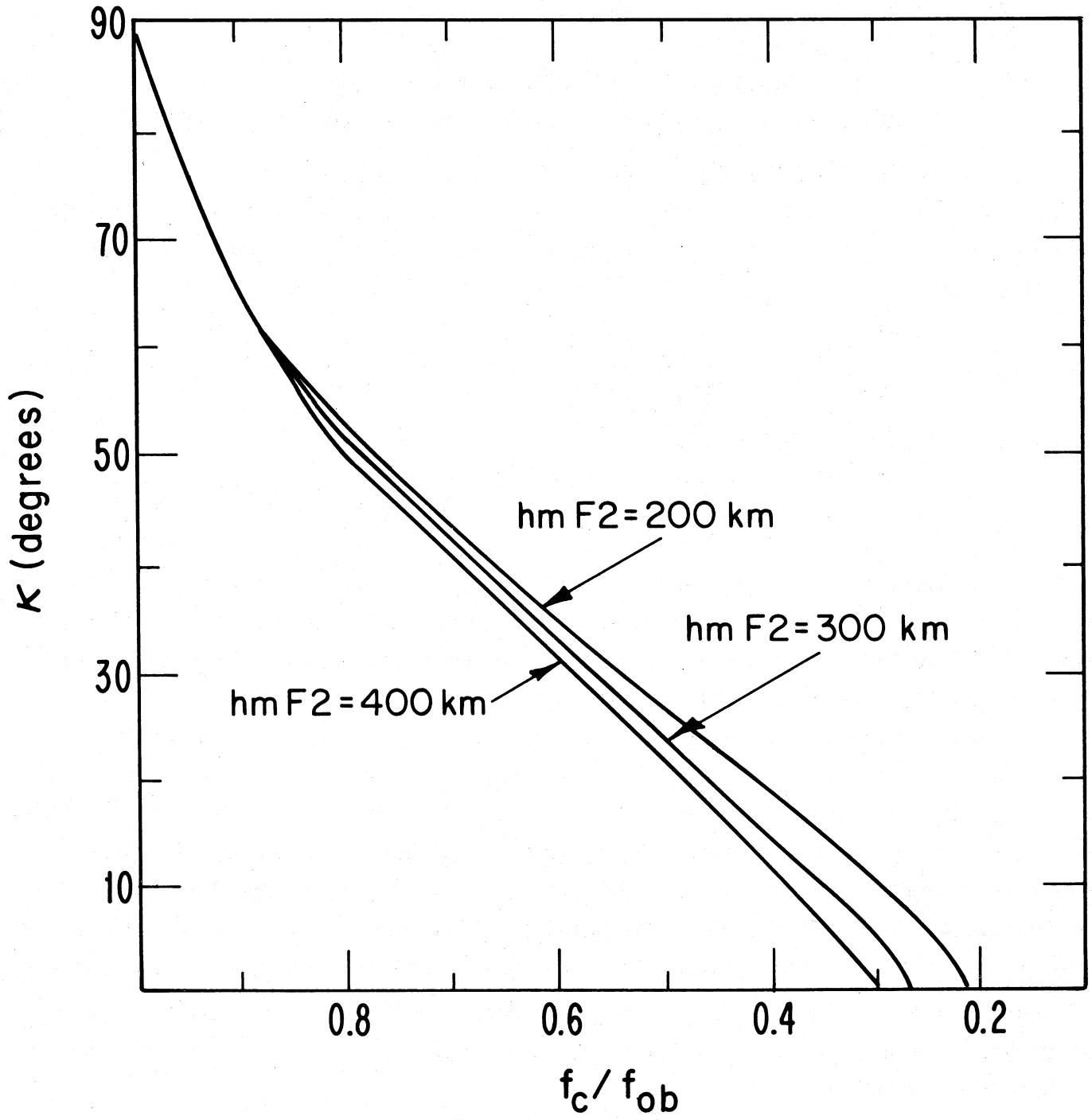

Figure 1. Values of take-off angle (κ) as a function of f_c/f_{ob}.

due caution and full awareness of the effect of the structure of the ionosphere on the observations.

3. DMSP HF RADIO NOISE CHARACTERISTICS

The DMSP satellite that is equipped with an HF noise receiver is typical of U. S. Air Force defense meteorological satellites. The satellite was launched in the late Spring of 1977 into a polar, almost sun-synchronous dawn-dusk orbit at about 800 km in altitude [Rush et al., 1978]. The HF noise receiver provides values of the logarithm of the receiver output voltage at the satellite in 100 kHz steps between the frequencies 1.2 and 13.9 MHz. The receiver continuously steps through the 128 frequency channels in a total time of 32 seconds. A value of the signal level in each 100 kHz bin is obtained once every 32 seconds (approximately 200 km along the satellite orbit). The receiver therefore dwells at each frequency for 0.25 seconds. The receiver has a dynamic range of 60 dB. The length of the antenna used with the receiver is limited by operational considerations. The effective length of the antenna in the ionospheric plasma is on the order of one meter. The satellite is equipped with a recording system enabling observations of radio noise to be made continuously along the satellite orbit.

Figure 2 gives an example of the HF noise signal strength as a function of frequency. The receiver output voltage has been deduced by using the equation derived from pre-launch calibration procedures [Rush et al., 1978]:

$$E = 10^{\left[\frac{N - 282.5}{52.5}\right]}$$

where

E = the terminal voltage and

N = the number of counts.

Shown in the figure is the receiver voltage as a function of frequency during a full scan of the receiver when the satellite was located at 40.4° North latitude and 265.8° East longitude at 12.6 hours Universal Time (UT) on July 27, 1977. It is readily apparent that the data at the higher end of the frequency scale, are more erratic than at the lower end. This is characteristic of the behavior of radio noise in the topside ionosphere. At frequencies above the sub-satellite ionospheric critical frequency, electromagnetic energy of terrestrial origin can penetrate the ionosphere from below and can be received at the satellite. The ragged or erratic spectrum at the high-frequency end of the figure (and greater than f_c) is due to electromagnetic energy at different frequencies being received at the satellite from various sources on the earth's surface.

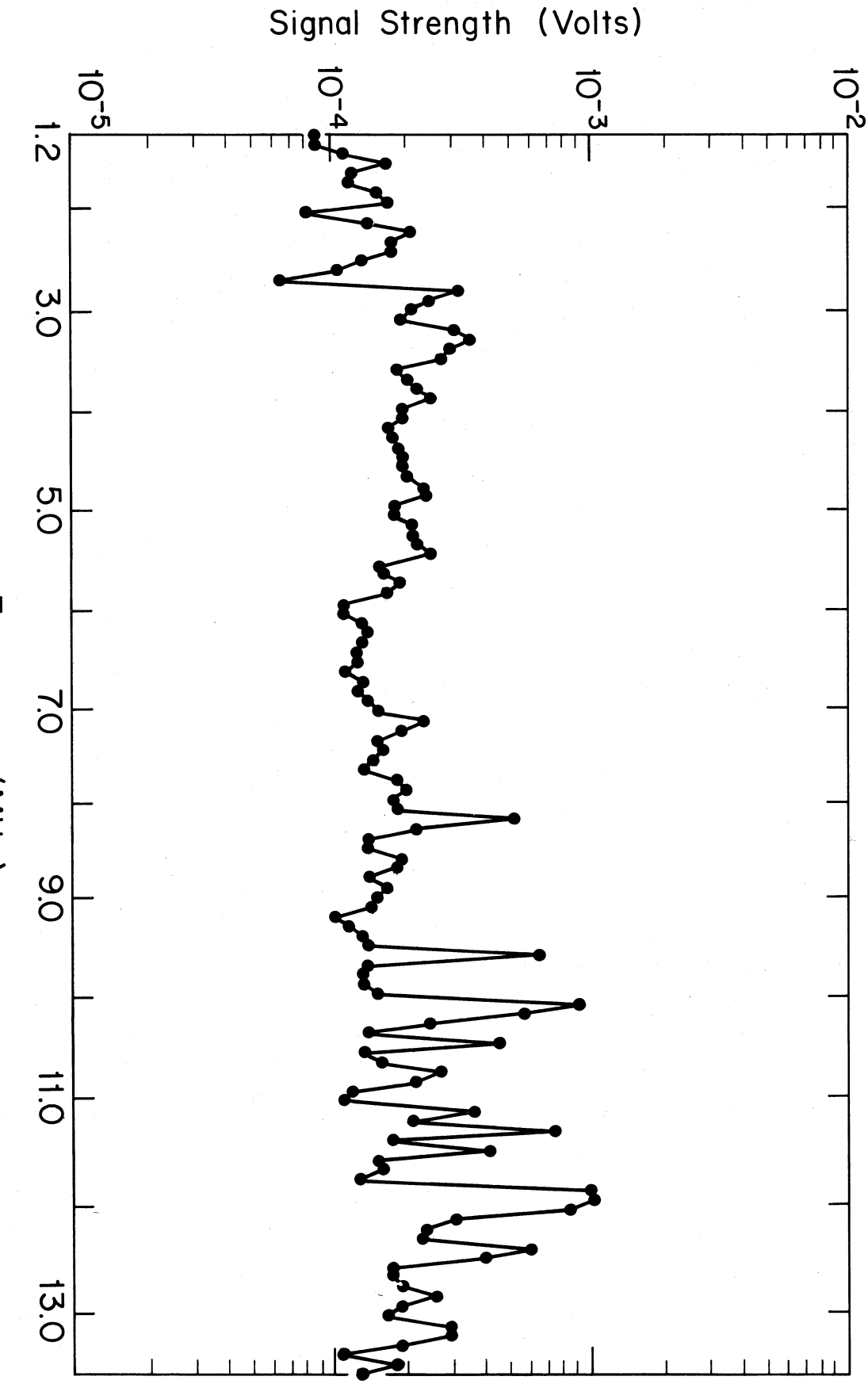

Figure 2. Signal strength (in volts) as a function of frequency observed by the DMSP satellite at 40.4°N, 265.8°E on July 27, 1977.

The cause of the relative enhancement in signal strength at the low frequency end (about 3.0 MHz) of the spectrum is not definitely known. It is worthwhile pointing out, however, that the critical frequency of the F2 region is believed to be on the order of 3.0 to 3.3 MHz for this time and location. These values are based on the method for predicting median values of foF2 given by the CCIR in Report 340-3 (CCIR, 1978). Thus, the large enhancement near 3.0 could be the result of radio energy slightly above the critical frequency being received at the satellite. The ragged nature of the frequencies below 3.0 MHz is somewhat puzzling, and may be due to contamination in the receiver from other sources at the satellite. In order that the conclusions derived from this study not be vitiated by data that may be of questionable accuracy, results are presented only for frequencies of 4.0 MHz and greater.

The base level of the spectrum shown in Figure 2 is somewhat higher than would be expected from an HF receiver in the topside ionosphere since the background level is anticipated to be the result of galactic noise alone. The enhanced base level observed could be due to the fact that the satellite itself is in a noisy environment and broadband noise could be generated by other instrumentation on-board the spacecraft. For these reasons, and because only receiver output voltages are available rather than field strength or antenna noise factor, the studies reported here have concentrated on discussing the morphological behavior of topside noise in relative rather than absolute terms.

4. DATA ANALYSIS METHODS

The observations of radio noise obtained by the DMSP satellite are stored on the tape recorder on-board the spacecraft and are read-out at specific ground stations according to a pre-selected format that is determined by operational Air Force considerations. The data used in this study have been obtained from the Air Force Geophysics Laboratory (AFGL). In order to study in detail the morphological behavior of the HF radio noise in the ionosphere above the F2 peak, it is necessary that maximum flexibility with regard to data presentation and analysis be maintained. It was, therefore, decided to analyze the data in terms of monthly increments while, maintaining enough flexibility in the analysis programs so that data from consecutive months could be readily combined and data from time periods that are less than a month could be easily processed.

The data for a given month were processed on a large computer and stored according to frequency (128 frequency bins corresponding to the 100 kHz separation from 1.2 to 13.9 MHz), local time (dawn or dusk), and sub-satellite geographic

latitude and longitude. Each month of data is equivalent to nearly one billion bits of information. A data processing program was developed that enabled the observations to be grouped in frequency and location. It was decided that observations within a five-degree latitude and longitude interval would be averaged together. The average value for each five-degree latitude-longitude interval, as well as the variance, standard deviation and standard error of the mean were determined and given routinely as output for each frequency bin. The standard deviation and standard error of the mean permit an assessment to be made as to just how representative the average values are of a general population. In addition to grouping data in frequency intervals, the processing program permitted data obtained on different days within the month to be grouped over a specified number of days.

5. RESULTS OF THE DATA ANALYSIS

The data obtained by the DMSP satellite were analyzed using the program described in the previous section. Various studies were undertaken in order to determine the behavior of HF radio noise in the topside ionosphere as a function of time interval over which data were averaged, as a function of frequency and as a function of sub-satellite location.

5.1. Time Interval Averaging

In order to obtain an indicator of how the HF radio environment at satellite altitude looks on a global scale, it is necessary to analyze data from successive orbits and successive days. Because the DMSP satellite is in nearly sun-synchronous dawn-dusk orbit, it is possible by combining data from successive morning or evening passes to obtain global maps of the noise environment since the satellite returns to the same general orbital position (apart from changes associated with orbital precession) every 24 hours. In the course of one day, however, only between 12 and 14 orbits of data are obtained for the dawn and dusk period over the entire globe. To construct global maps of the radio noise, it was necessary to average data over several days of observation. An investigation was, therefore, undertaken to study the number of consecutive days of data that were needed to produce noise values at each frequency and at each five-degree latitude-longitude increment. Looking at plots of the satellite orbit, it became apparent that at least five days of consecutive data were needed to provide sufficient coverage to construct global maps of the HF radio noise in the topside ionosphere. It was necessary to determine if the noise values deduced from as little as 5 day's data were representative of the noise environment.

The global behavior of the HF noise at specific frequencies was studied for data averaged over 5, 10, and 15 days. Table 1 shows the average value of the radio noise (in receiver counts, N) and the associated standard deviation for two frequencies, 8.5 and 11.7 MHz, observed during November 1977. In the table, results are shown for 5, 10, and 15-day averages centered on 15 November 1977 for five different locations over the globe. The results indicate that there is no significant difference between averages deduced from 5, 10, or 15 day's of data. However, most of the global studies undertaken as part of this effort involved data observed over one, two, or three month periods.

5.2. Global Maps of HF Radio Noise

Global maps of the radio noise at specific frequencies have been produced for the dawn and dusk time periods. Figure 3 shows the global distribution of radio noise observed at 12 MHz during the dawn period of September, October, and November, 1977. The figure displays contours of receiver terminal voltage expressed in millivolts. In viewing the figure, it should be borne in mind that the contours represent the average noise intensity observed during the three-month period of September, October, and November, 1977, and because of the satellite orbit, the time of the Observations centers around local dawn over the entire globe. In Figure 3 and those that follow, the areas designated as "MAX" refer to those areas in which the receiver saturated; i.e., the signal strength reached a level of 1.1 millivolts at the satellite height.

From the figure, a number of features are immediately obvious. The highest values of the contours are associated with land areas. The region above the European-Asian continent and the region above the easternmost part of Asia show the most intense noise levels. Centers of relatively high values of noise can be discerned above the east and west coasts of the United States and Central America. Areas of somewhat lesser noise values, yet still relatively intense, can be seen above southern Africa, Australia, and eastern South America. The ocean areas show little relative noise intensity. The general pattern of the observed HF environment during the dusk period departs very little from that displayed in Figure 3 and for this reason is not shown here.

It is somewhat surprising that the results presented in Figure 3 do not show relative increases in the radio environment above the tropical regions. It is well documented (Crichlow et al., 1971, for example) that the areas of highest atmospheric noise intensity occur in the land areas of the tropics. There is no evidence of systematic intense radio noise in the tropical regions seen in any of the results studied in this investigation. Apart from the lack of an increase in the radio

Table 1. Values of HF Receiver Counts for 8.5 and 11.7 MHz Averaged Over 5, 10, and 15 Day Intervals

Geographic Location	8.5 MHz 5 Day	8.5 MHz 10 Day	8.5 MHz 15 Day	11.7 MHz 5 Day	11.7 MHz 10 Day	11.7 MHz 15 Day
DAWN						
47° N, 47° E	64 ± 1	55 ± 8	65 ± 16	123 ± 1	124 ± 3	124 ± 2
47° N, 277° E	44 ± 4	44 ± 3	45 ± 3	101 ± 7	104 ± 7	102 ± 7
12° N, 2° E	37 ± 1	37 ± 1	35 ± 2	57 ± 1	57 ± 1	56 ± 1
22° S, 292° E	38 ± 2	38 ± 2	38 ± 2	57 ± 1	57 ± 1	56 ± 2
47° S, 87° E	39 ± 7	39 ± 2	39 ± 2	57 ± 1	55 ± 1	56 ± 2
DUSK						
Geographic Location	8.5 MHz 5 Day	8.5 MHz 10 Day	8.5 MHz 15 Day	11.7 MHz 5 Day	11.7 MHz 10 Day	11.7 MHz 15 Day
47° N, 47° E	63 ± 1	63 ± 1	63 ± 1	123 ± 1	123 ± 1	123 ± 1
47° N, 277° E	50 ± 4	49 ± 3	49 ± 3	105 ± 2	98 ± 7	98 ± 7
12° N, 2° E	34 ± 2	36 ± 3	36 ± 3	55 ± 1	56 ± 2	56 ± 2
22° S, 292° E	36 ± 3	36 ± 4	36 ± 3	57 ± 1	57 ± 1	56 ± 1
47° S, 87° E	37 ± 2	38 ± 2	38 ± 3	65 ± 1	64 ± 2	62 ± 3

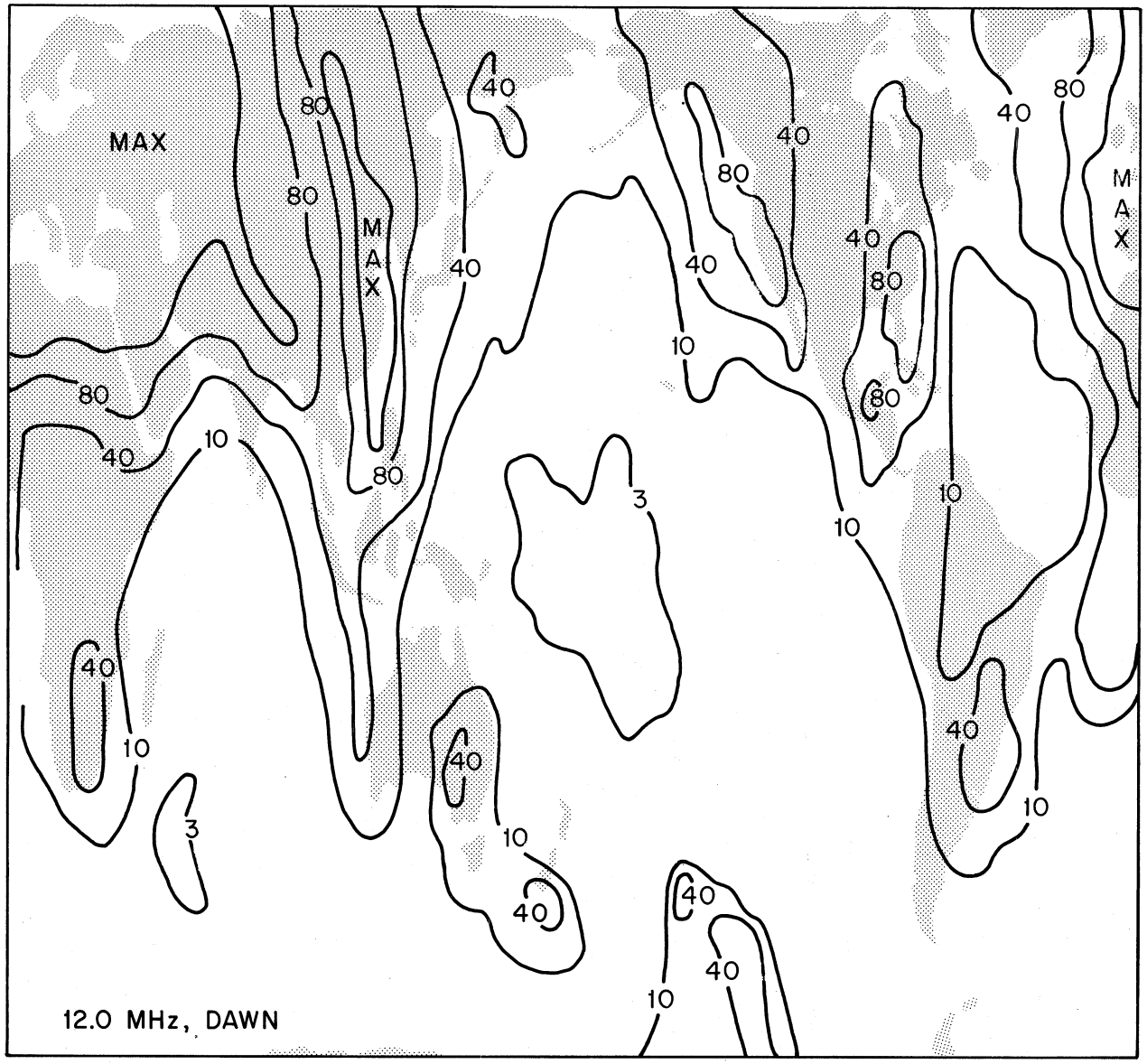

Figure 3. Global distribution of radio noise observed at 12 MHz during the dawn period of September-November 1977. Contours are receiver output voltage (millivolts $\times 10^{-2}$).

noise above the tropical regions, the results in Figure 3, in general, agree with those given by Herman et al. (1973, see their Figure 11) for the land areas even though our results are averaged over a three-month period (September, October, and November, 1977) and those of Herman et al. (1973) were deduced using approximately 120 data points obtained during a five-day period in December, 1977. The frequency given by Herman et al. (1973)--9.18 MHz--also differs from that of Figure 3.

Figures 4a and 4b show the global behavior of the HF noise observed at 11.8 MHz during dawn (Figure 4a) and dusk (Figure 4b) for a 30-day period centered on November 15, 1977. The same general features present in Figure 3 can be seen in Figures 4a and 4b. This is not too surprising since the frequency analyzed in Figure 3 is very close to that in Figure 4. Figures 5a and 5b and Figures 6a and 6b display similar results for frequencies of 9.6 and 6.0 MHz. The magnitude of the noise observed at 9.6 and 6.0 MHz generally is a little smaller than that seen in Figure 4a and 4b for 11.8 MHz, but the same general features persist.

Not all frequencies, however, display similar features. Figures 7a and 7b and Figures 8a and 8b show results obtained at 8.5 MHz and 12.5 MHz, respectively. The region above the European-Asian continent still displays the highest noise values, but the magnitude of the noise seen in Figures 7 and 8 are much less than those of Figures 3 through 6. The difference in the morphological behavior as a function of frequency is discussed in the next sub-section.

5.3. Frequency Dependence of HF Radio Noise

In an effort to illustrate the morphological behavior of the HF radio environment at satellite heights for various frequencies, Figures 9 through 13 depict the noise intensity observed during the dawn period and Figures 14 through 18 depict the noise intensity observed during the dusk period in 0.5 MHz increments beginning at 4.0 MHz and continuing to 13.5 MHz. On each of the figures, the HF radio environment observed when the satellite was orbiting above three different regions of the globe is presented: the Eurasian region (extending from 30°N to 70°N latitude and from 0° to 95°E longitude), the North American region (extending from 30°N to 70°N latitude and from 50°W to 145°W longitude), and the Australian region (extending from 10°S to 50°S latitude and from 85°E to 180°E longitude). As was the case for the previous Figure 5, the contours are given in millivolts and refer to data observed over the three-month period: September, October, and November, 1977. For those frequencies and regions of the globe that displayed little change in the value of the noise intensity over the entire region, a single contour approximating a circle has been drawn manually.

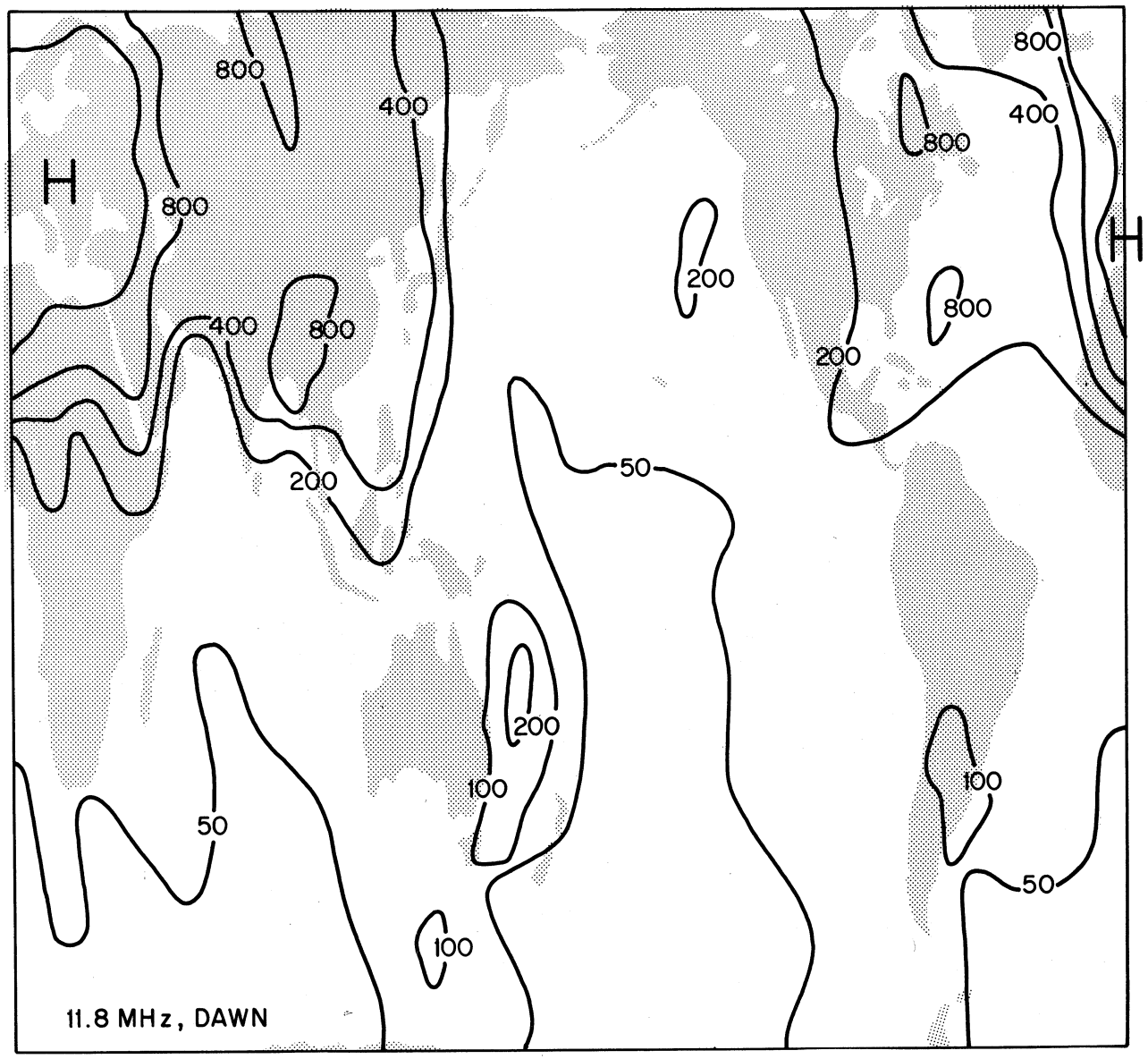

Figure 4a. Global distribution of radio noise observed at 11.8 MHz during the dawn period of November 1977. Contours are receiver output voltage (millivolts $\times 10^{-3}$).

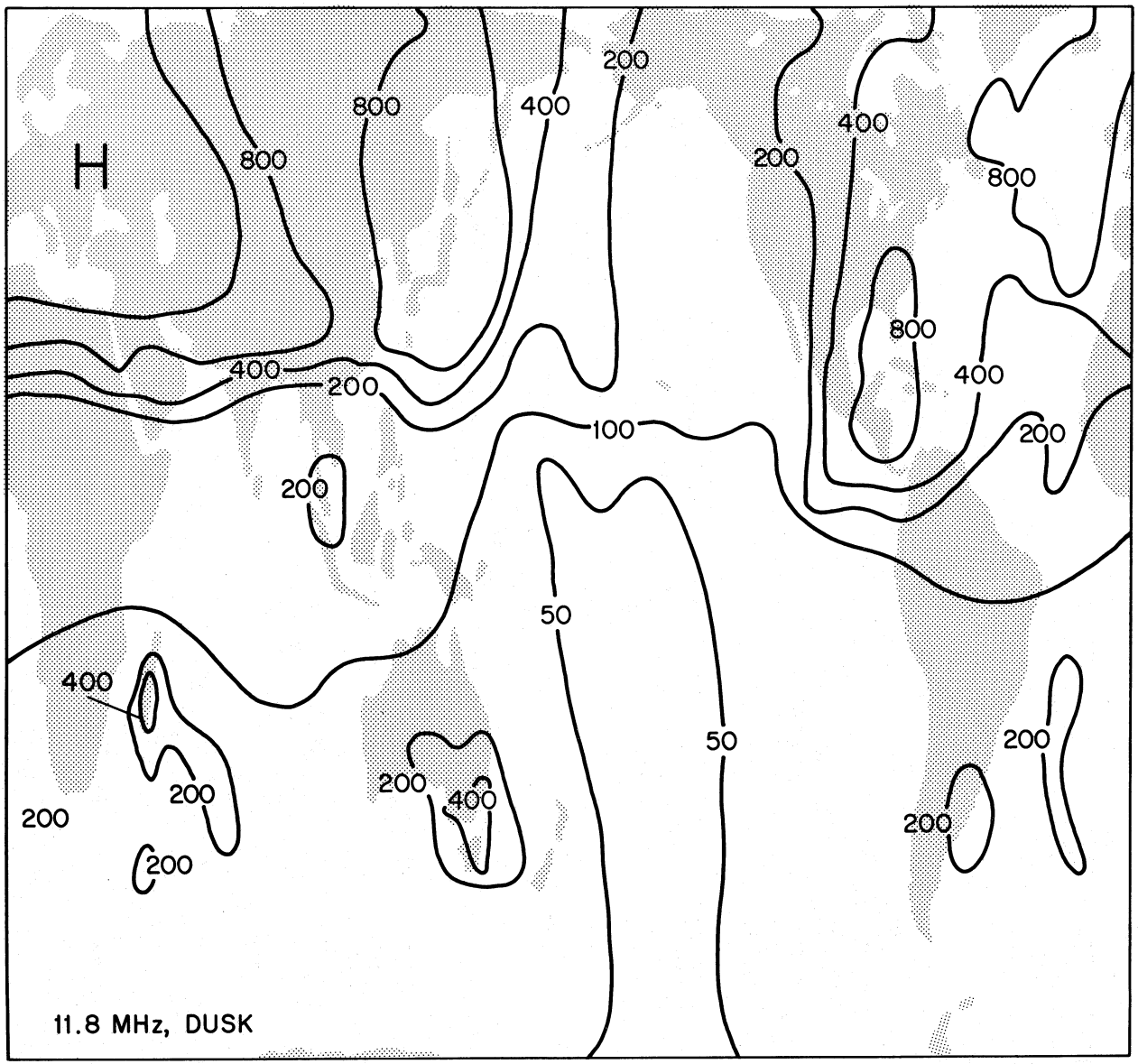

Figure 4b. Global distribution of radio noise observed at 11.8 MHz during the dusk period of November 1977. Contours are receiver output voltage (millivolts $\times 10^{-3}$).

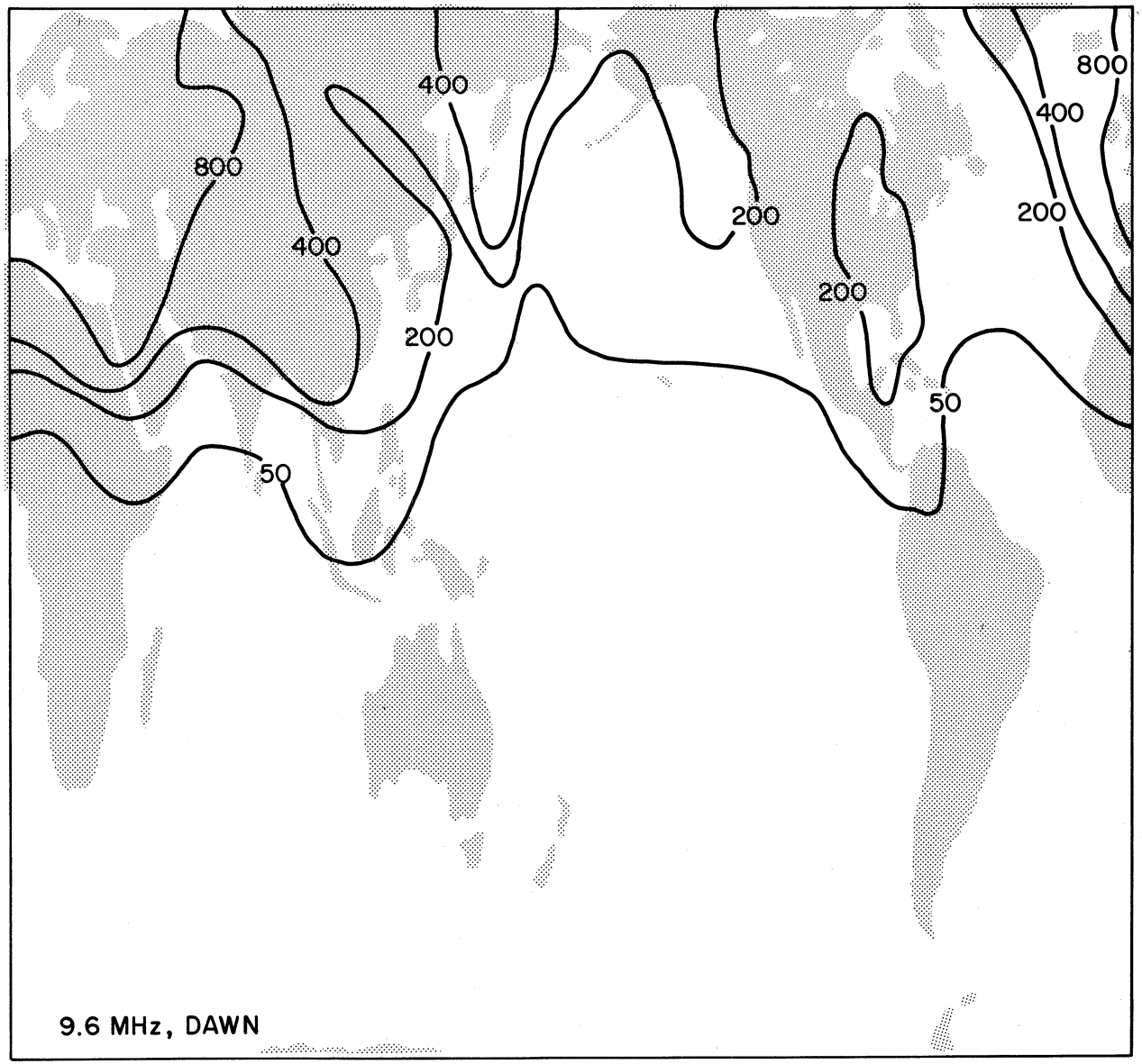

Figure 5a. Global distribution of radio noise observed at 9.6 MHz during the dawn period of November 1977. Contours are receiver output voltage (millivolts × 10^{-3}).

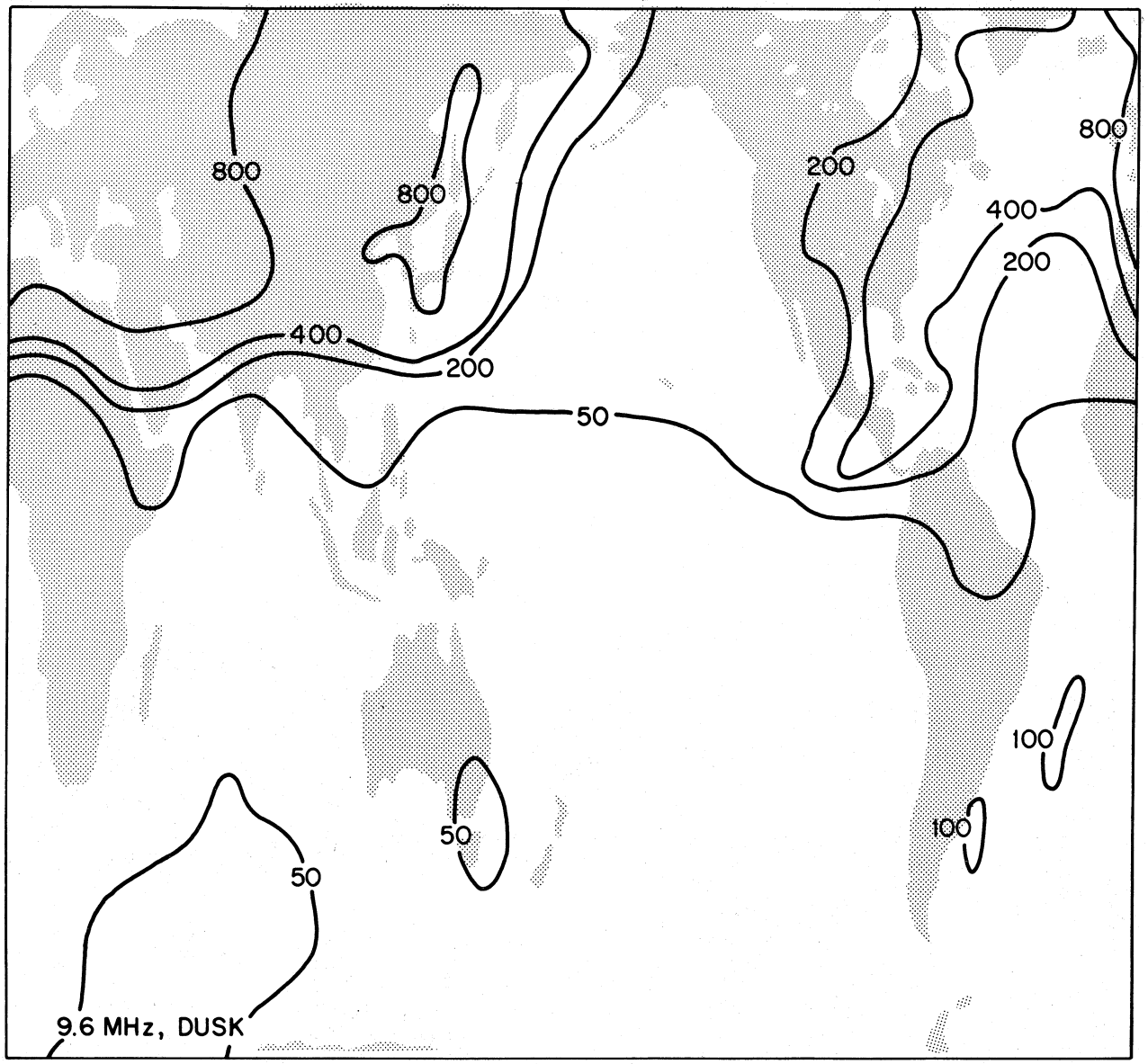

Figure 5b. Global distribution of radio noise observed at 9.6 MHz during the dusk period of November 1977. Contours are receiver output voltage (millivolts $\times 10^{-3}$).

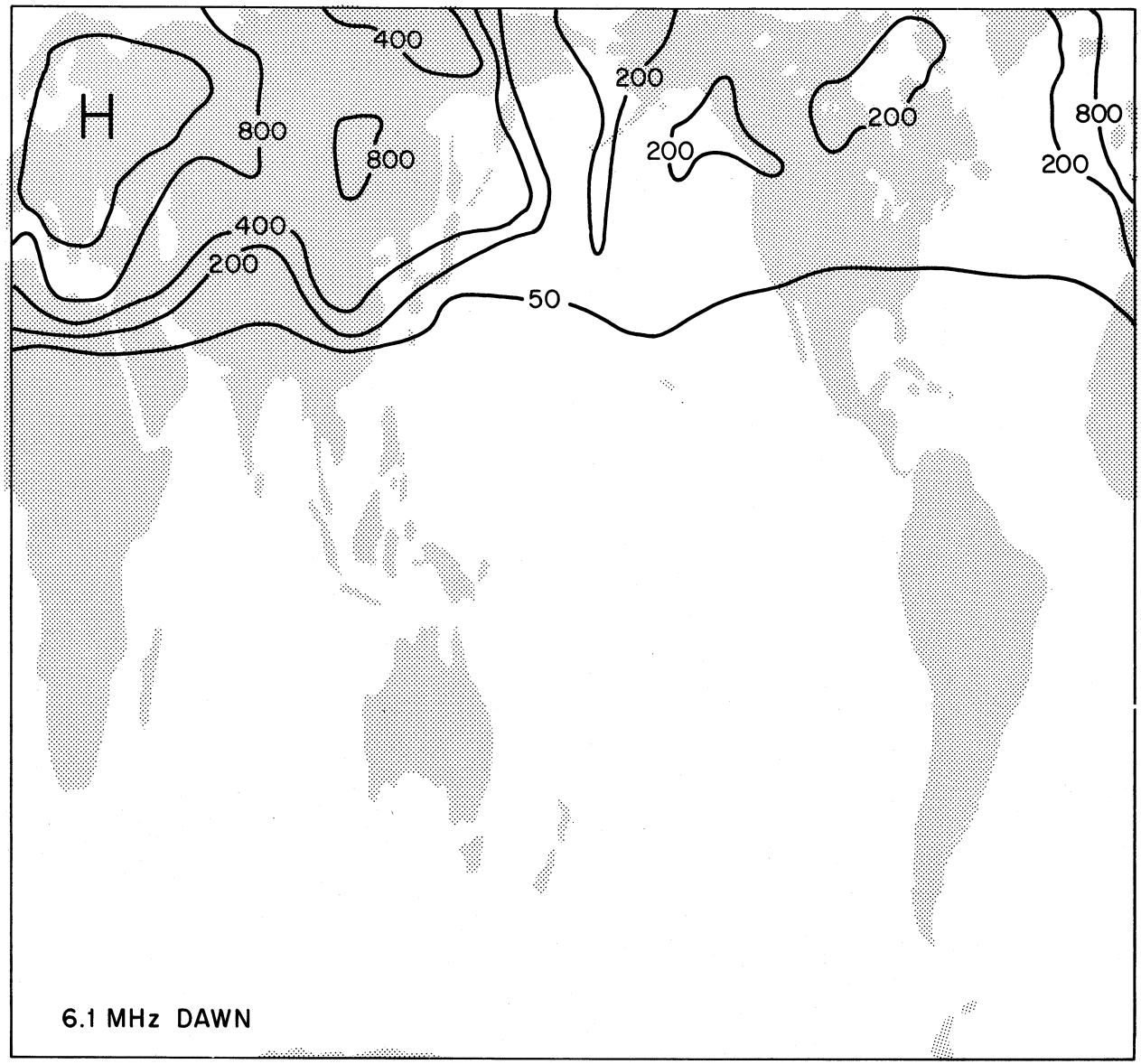

Figure 6a. Global distribution of radio noise observed at 6.1 MHz during the dawn period of November 1977. Contours are receiver output voltage (millivolts × 10^{-3}).

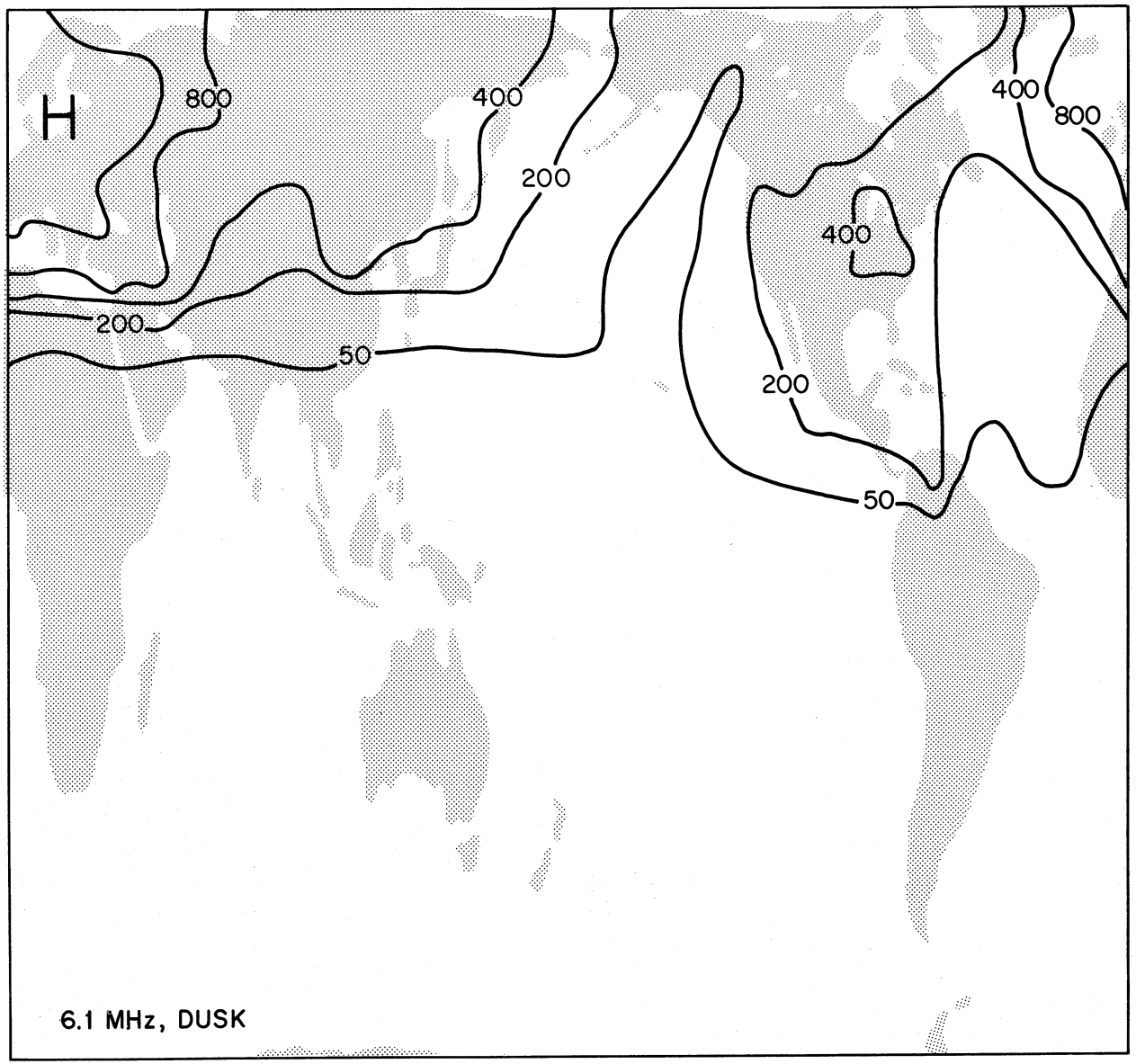

Figure 6b. Global distribution of radio noise observed at 6.1 MHz during the dusk period of November 1977. Contours are receiver output voltage (millivolts $\times 10^{-3}$).

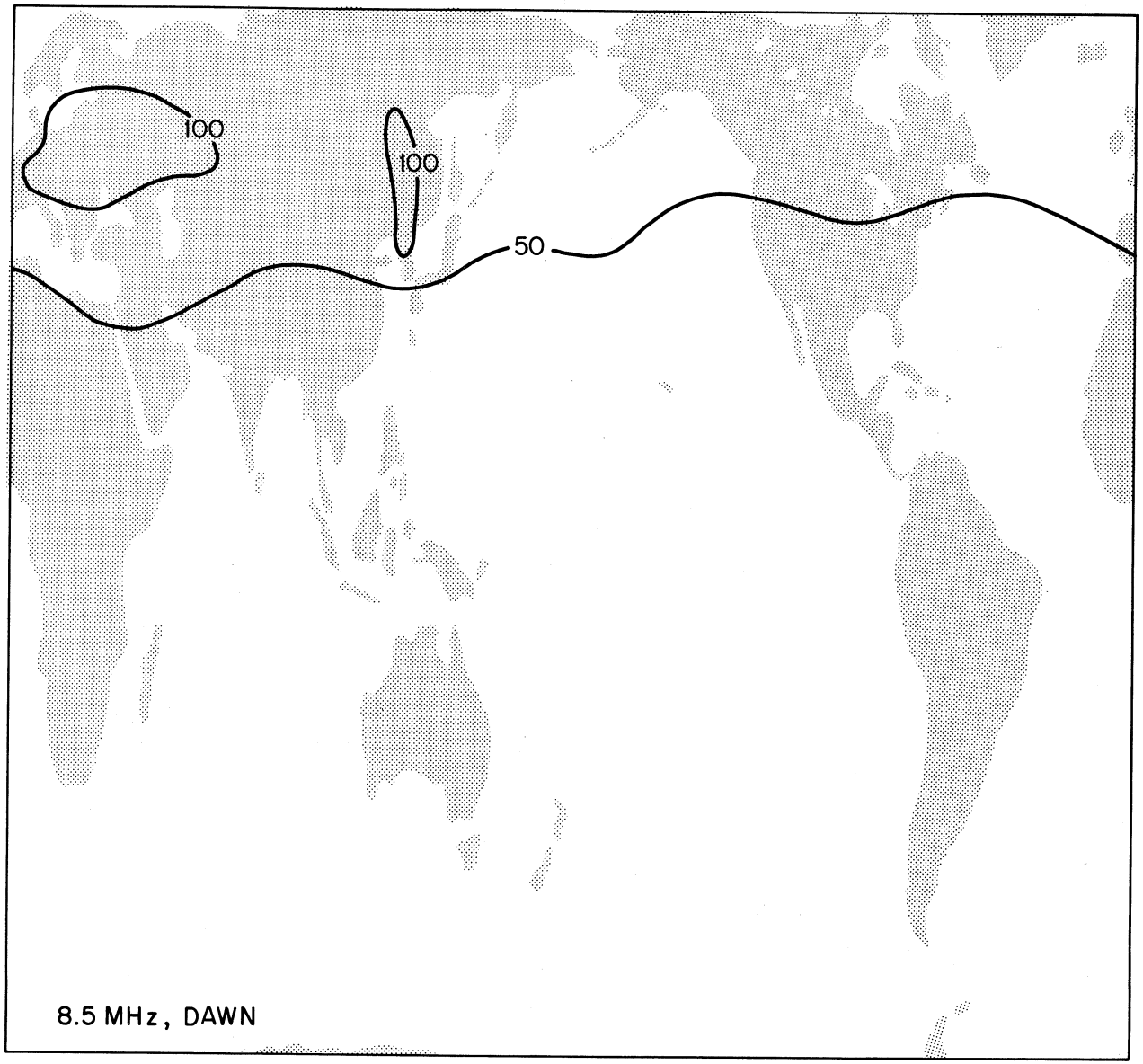

Figure 7a. Global distribution of radio noise observed at 8.5 MHz during the dawn period of November 1977. Contours are receiver output voltage (millivolts $\times 10^{-3}$).

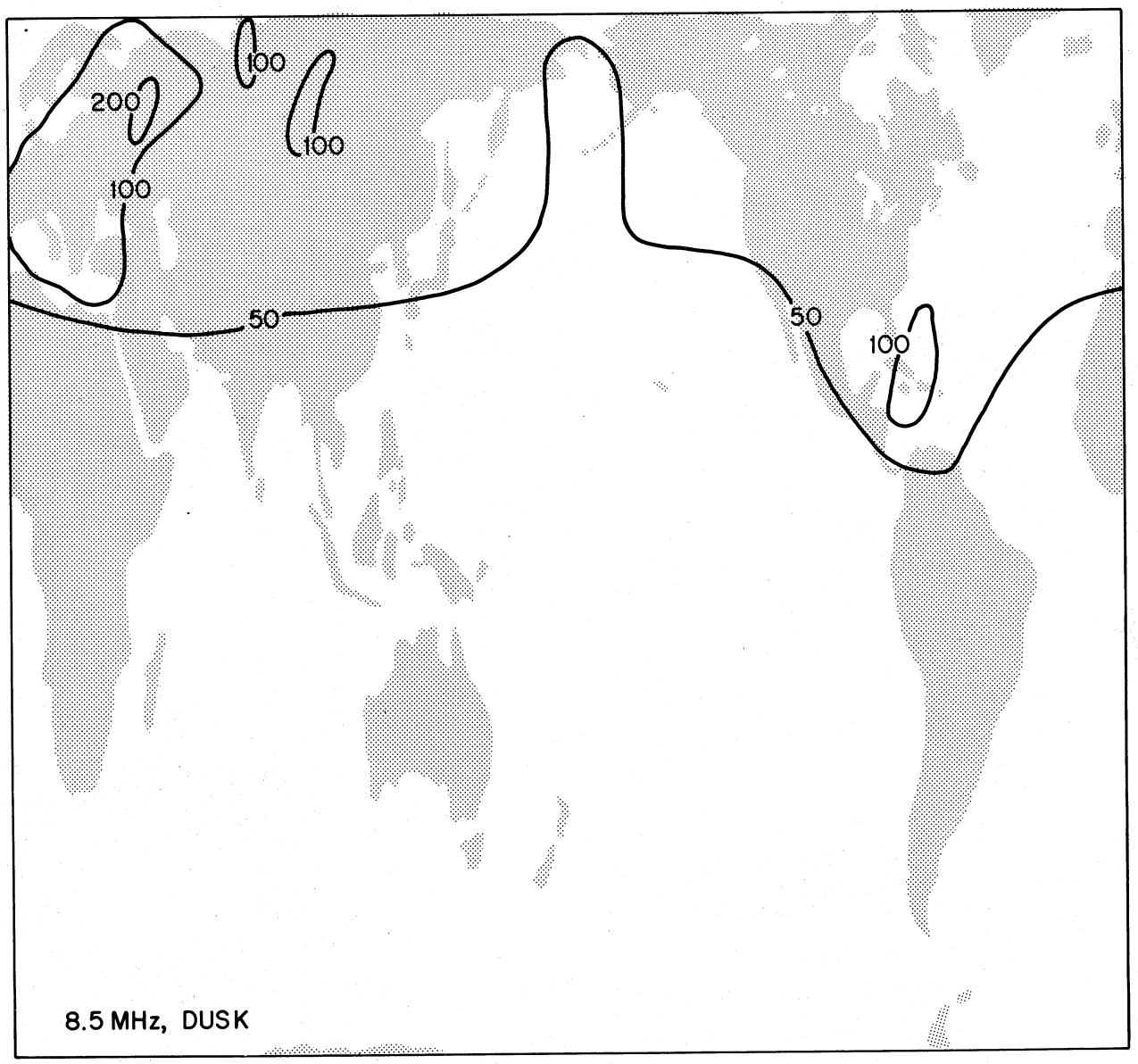

Figure 7b. Global distribution of radio noise observed at 8.5 MHz during the dusk period of November 1977. Contours are receiver output voltage (millivolts $\times 10^{-3}$).

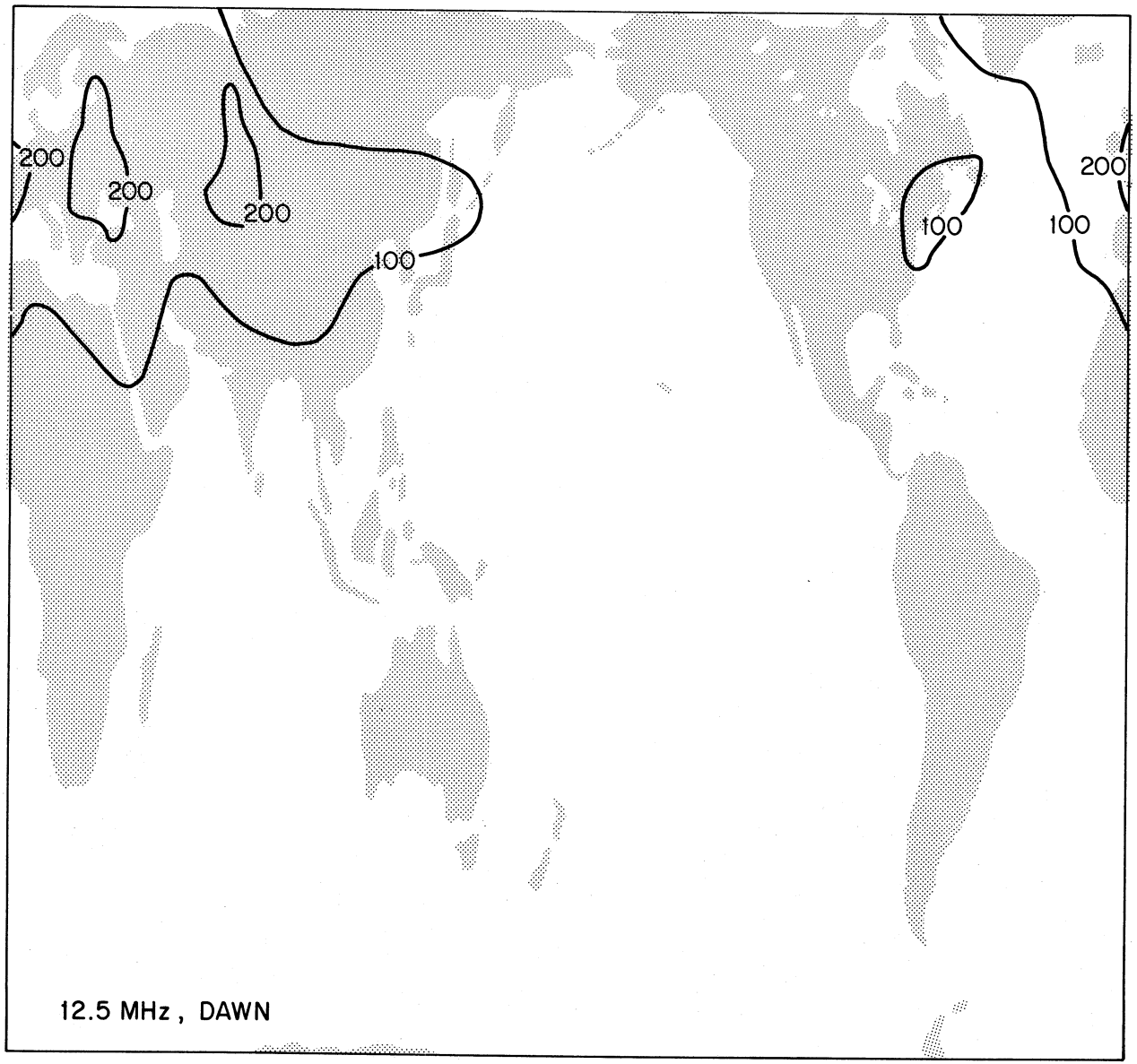

Figure 8a. Global distribution of radio noise observed at 12.5 MHz during the dawn period of November 1977. Contours are receiver output voltage (millivolts $\times 10^{-3}$).

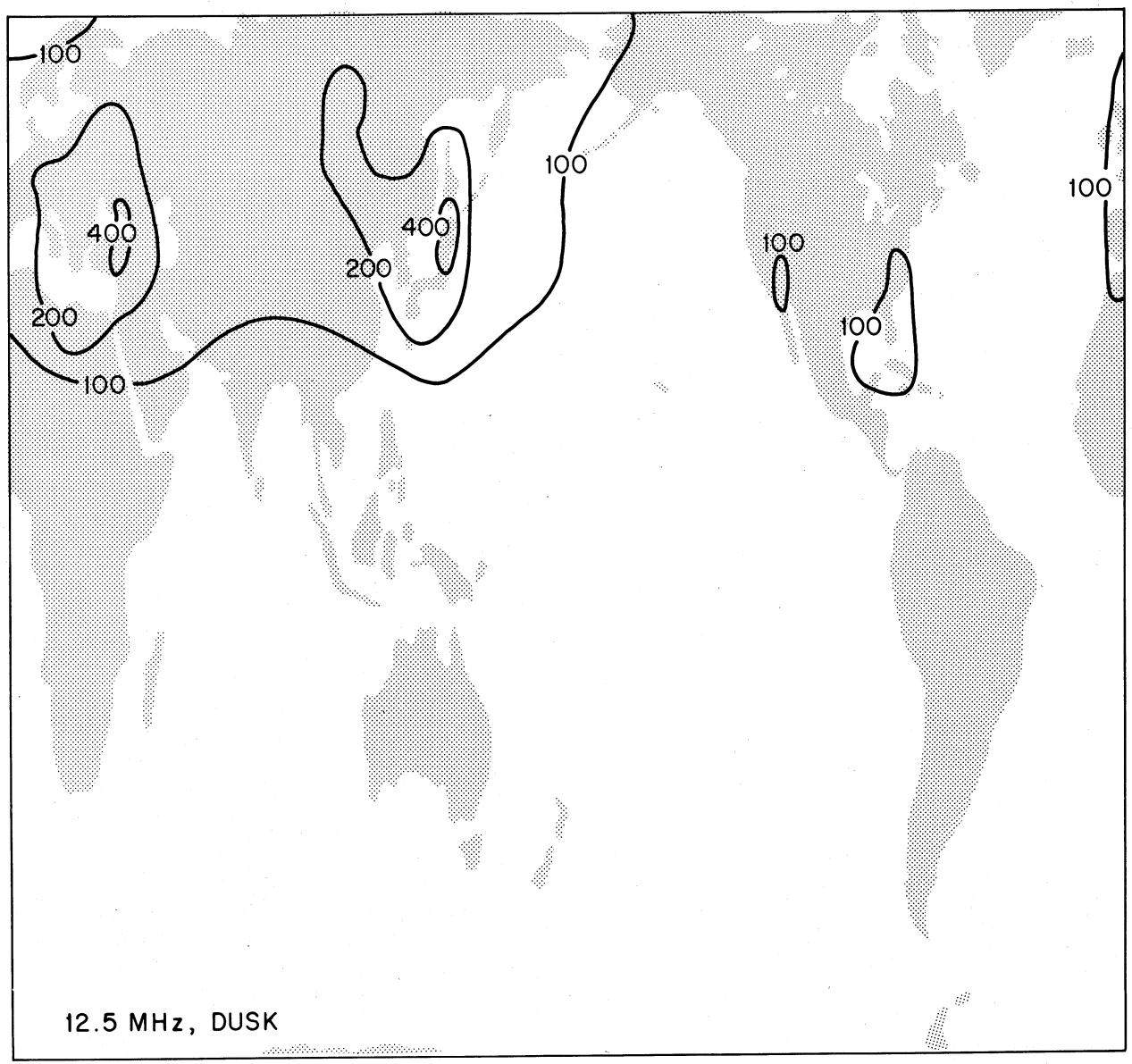

Figure 8b. Global distribution of radio noise observed at 12.5 MHz during the dusk period of November 1977. Contours are receiver output voltage (millivolts $\times 10^{-3}$).

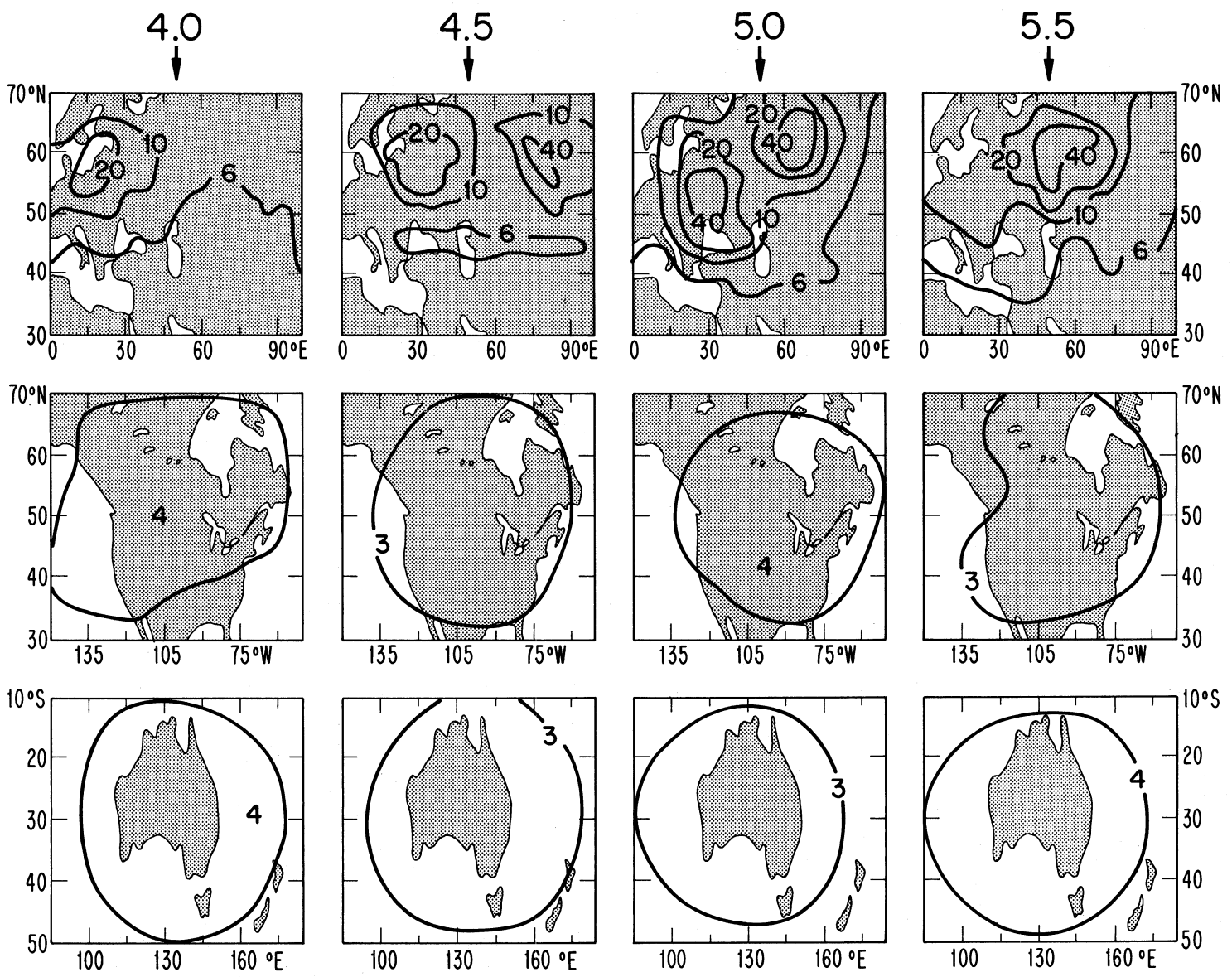

Figure 9. Behavior of the HF radio environment at local dawn above Eurasia, North America, and Australia for frequencies of 4.0, 4.5, 5.0 and 5.5 MHz during the period September-November 1977. Contours are receiver output voltage (millivolts × 10^{-2}).

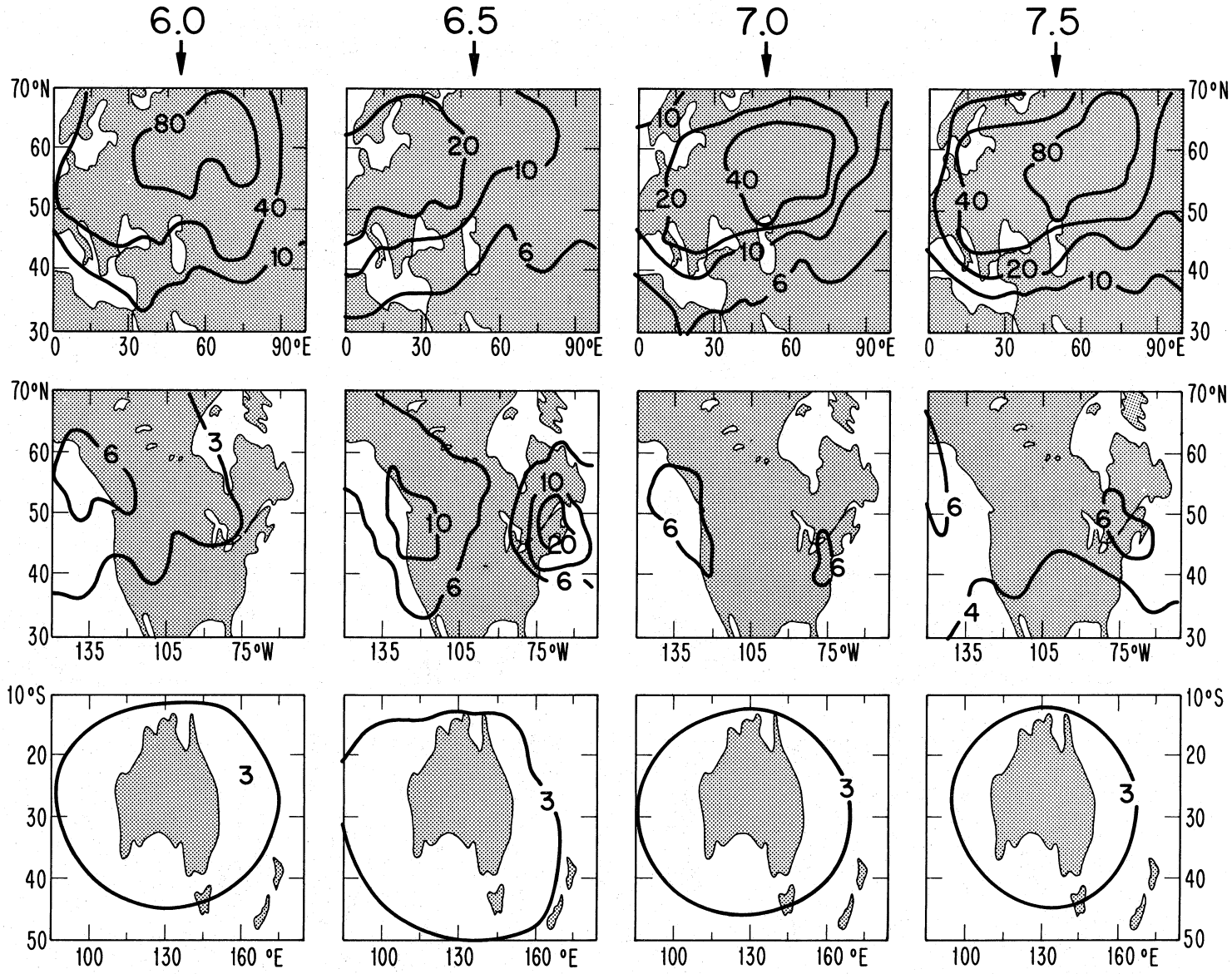

Figure 10. Behavior of the HF radio environment at local dawn above Eurasia, North America, and Australia for frequencies of 6.0, 6.5, 7.0, and 7.5 MHz during the period September-November 1977. Contours are receiver output voltage (millivolts $\times 10^{-2}$).

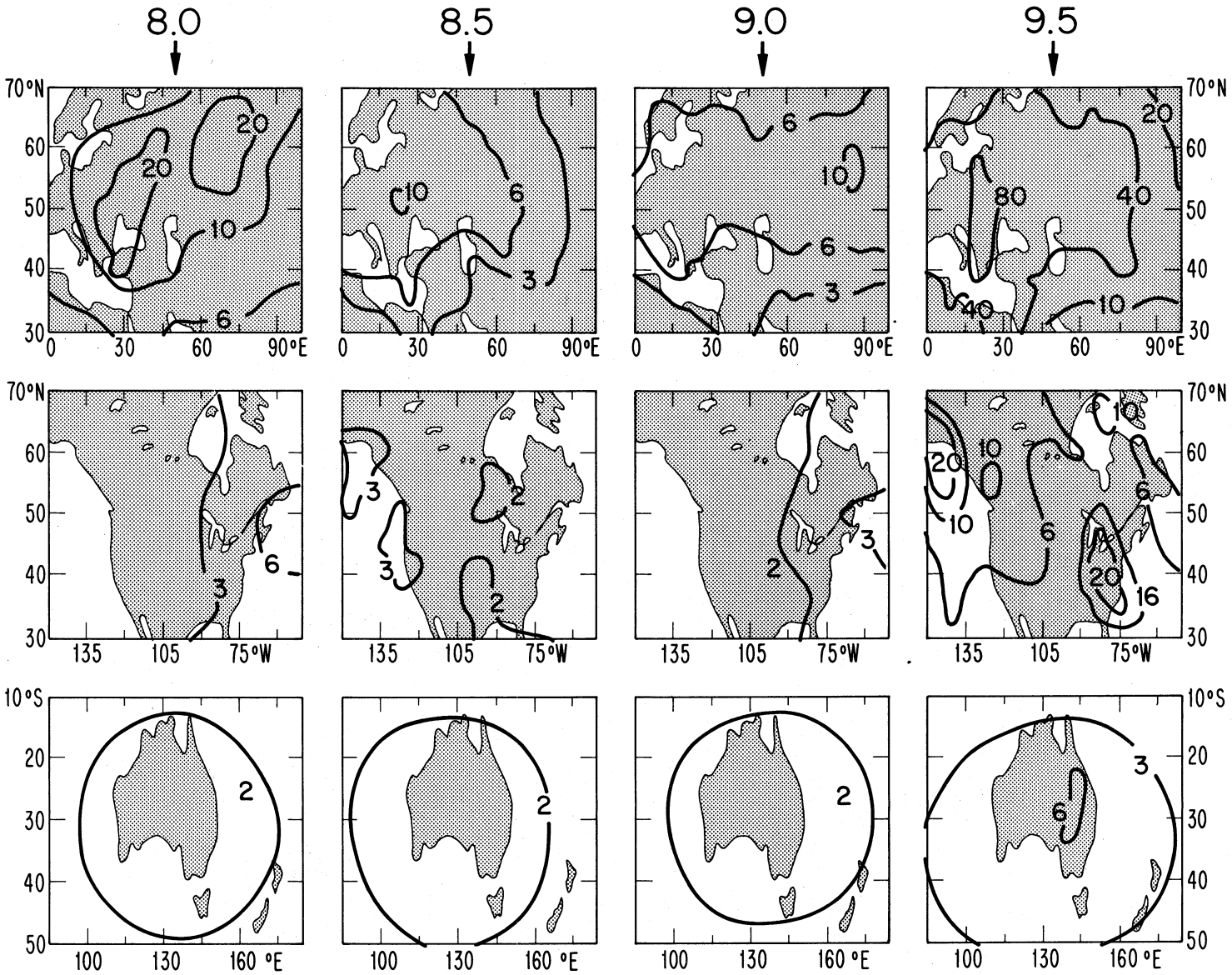

Figure 11. Behavior of the HF radio environment at local dawn above Eurasia, North America, and Australia for frequencies of 8.0, 8.5, 9.0, and 9.5 MHz during the period September-November 1977. Contours are receiver output voltage (millivolts × 10^{-2}).

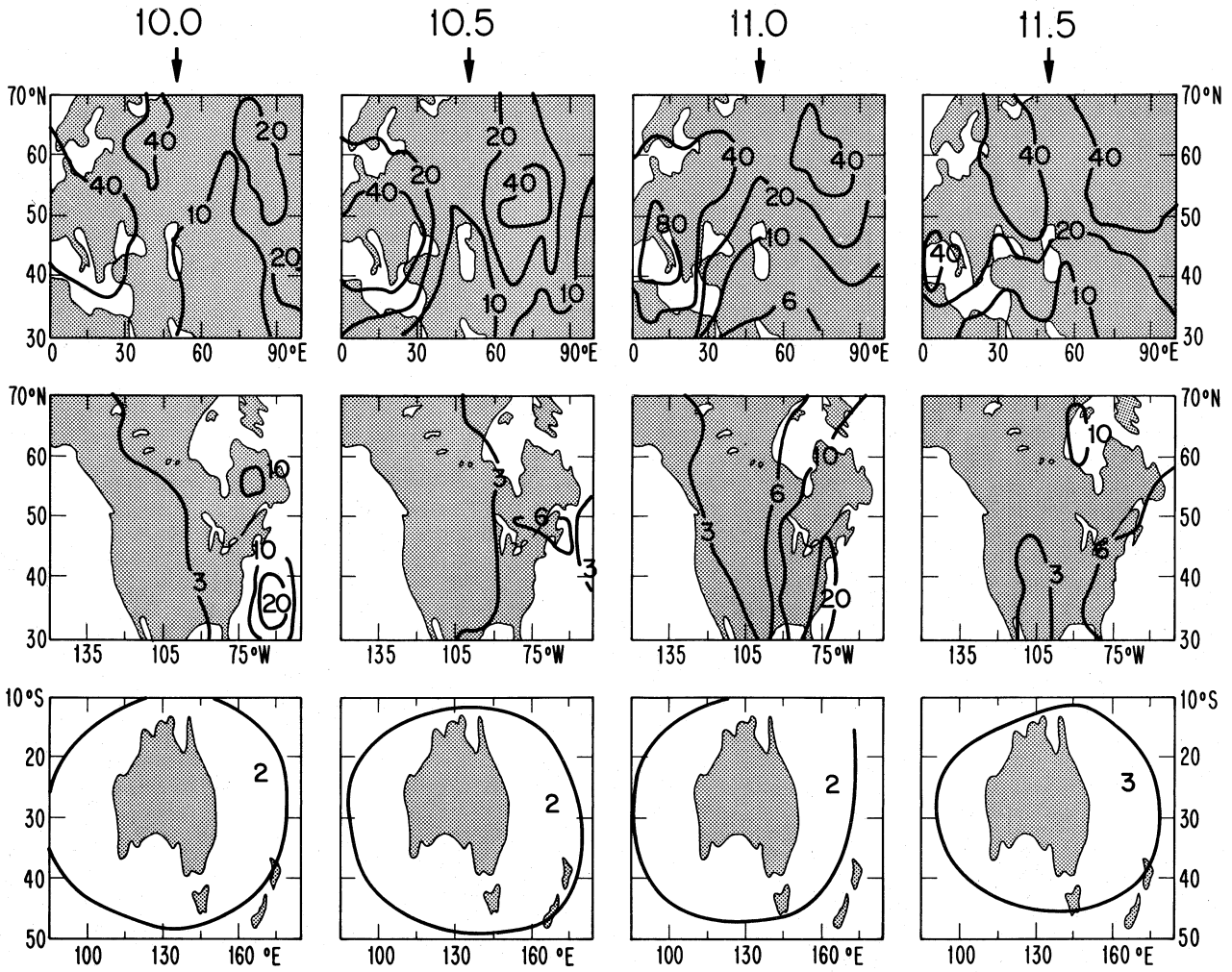

Figure 12. Behavior of the HF radio environment at local dawn above Eurasia, North America, and Australia for frequencies of 10.0, 10.5, 11.0, and 11.5 MHz during the period September-November 1977. Contours are receiver output voltage (millivolts × 10^{-2}).

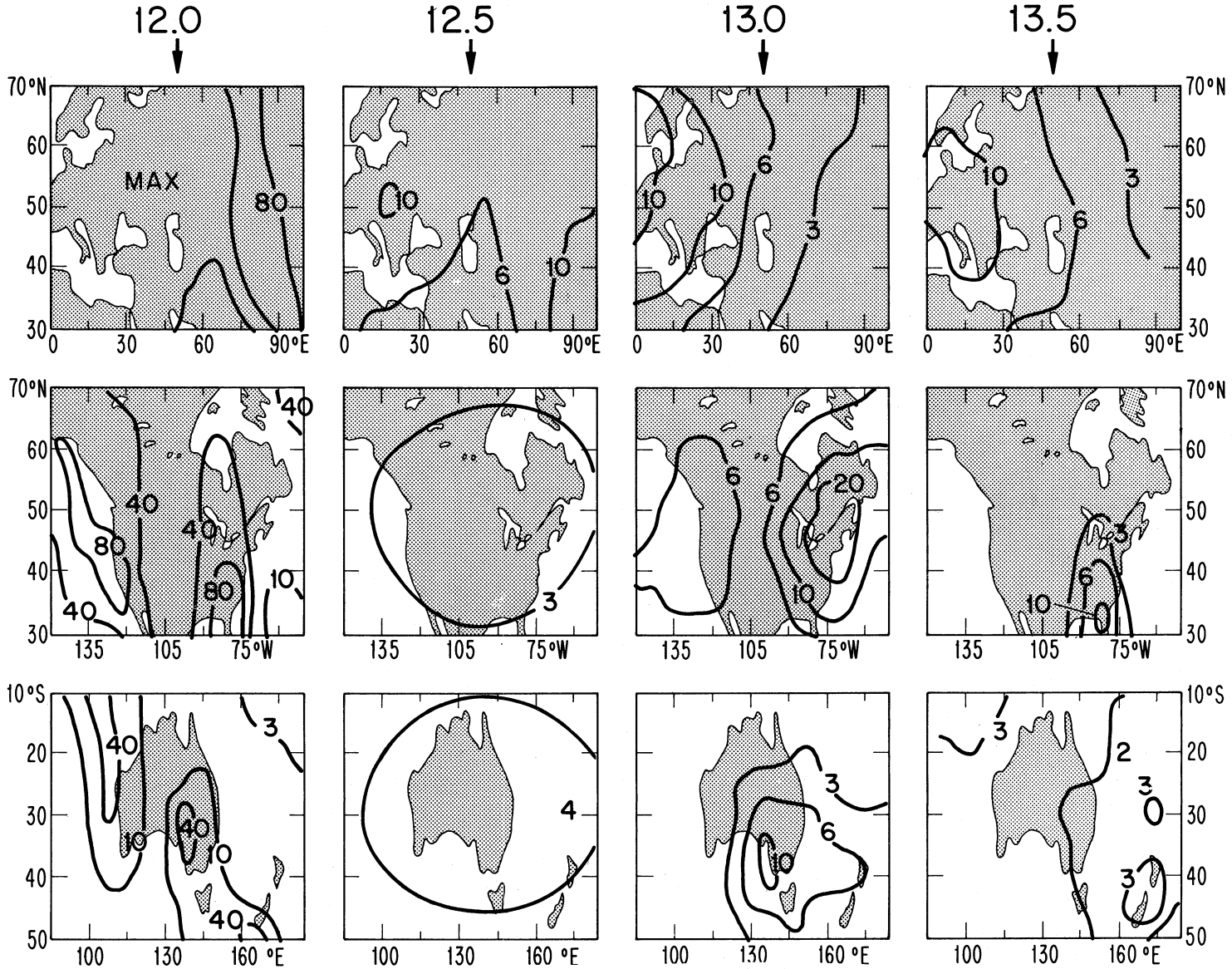

Figure 13. Behavior of the HF radio environment at local dawn above Eurasia, North America, and Australia for frequencies of 12.0, 12.5, 13.0, and 13.5 MHz during the period September-November 1977. Contours are receiver output voltage (millivolts $\times 10^{-2}$).

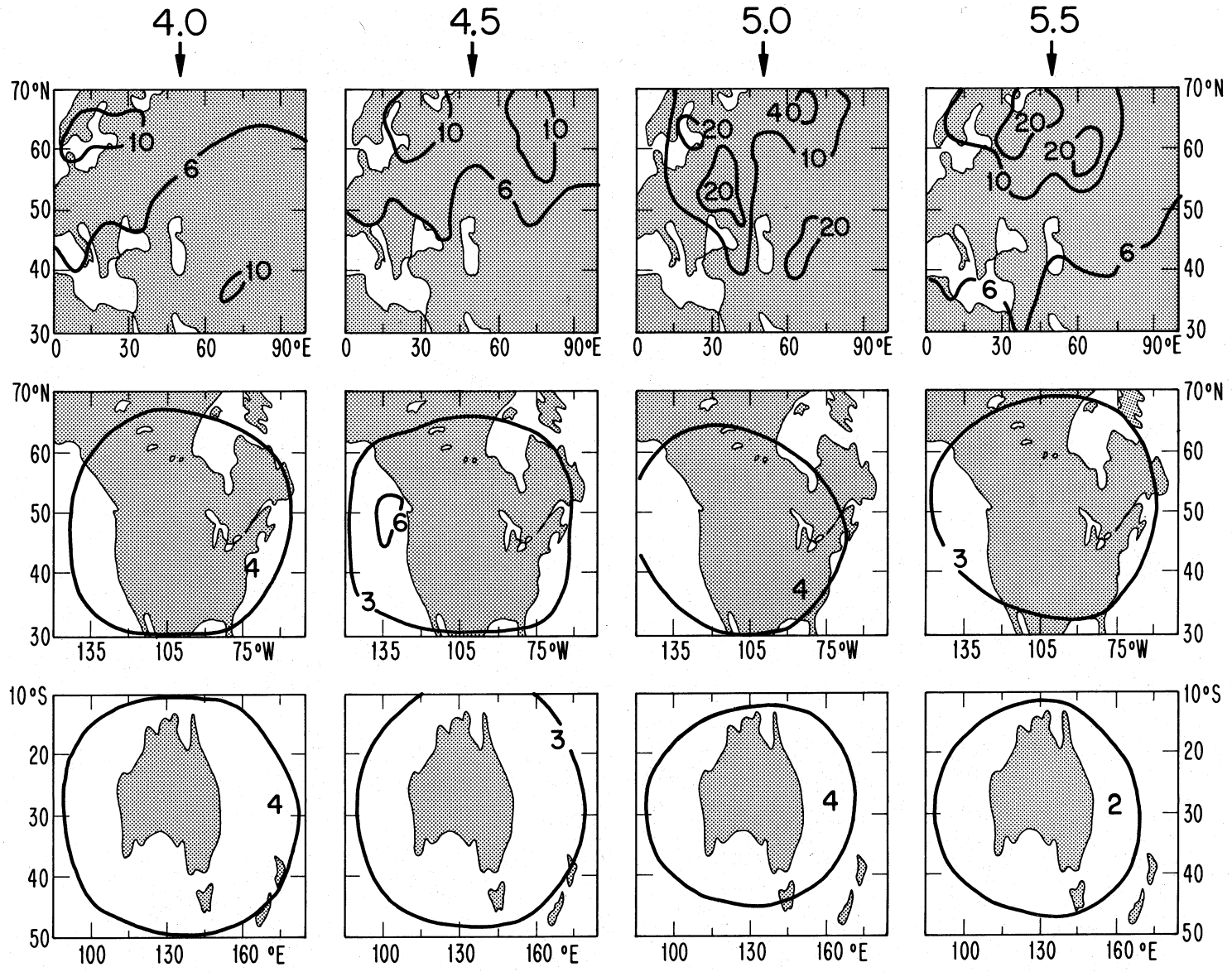

Figure 14. Behavior of the HF radio environment at local dusk above Eurasia, North America, and Australia for frequencies of 4.0, 4.5, 5.0, and 5.5 MHz during the period September-November 1977. Contours are receiver output voltage (millivolts × 10^{-2}).

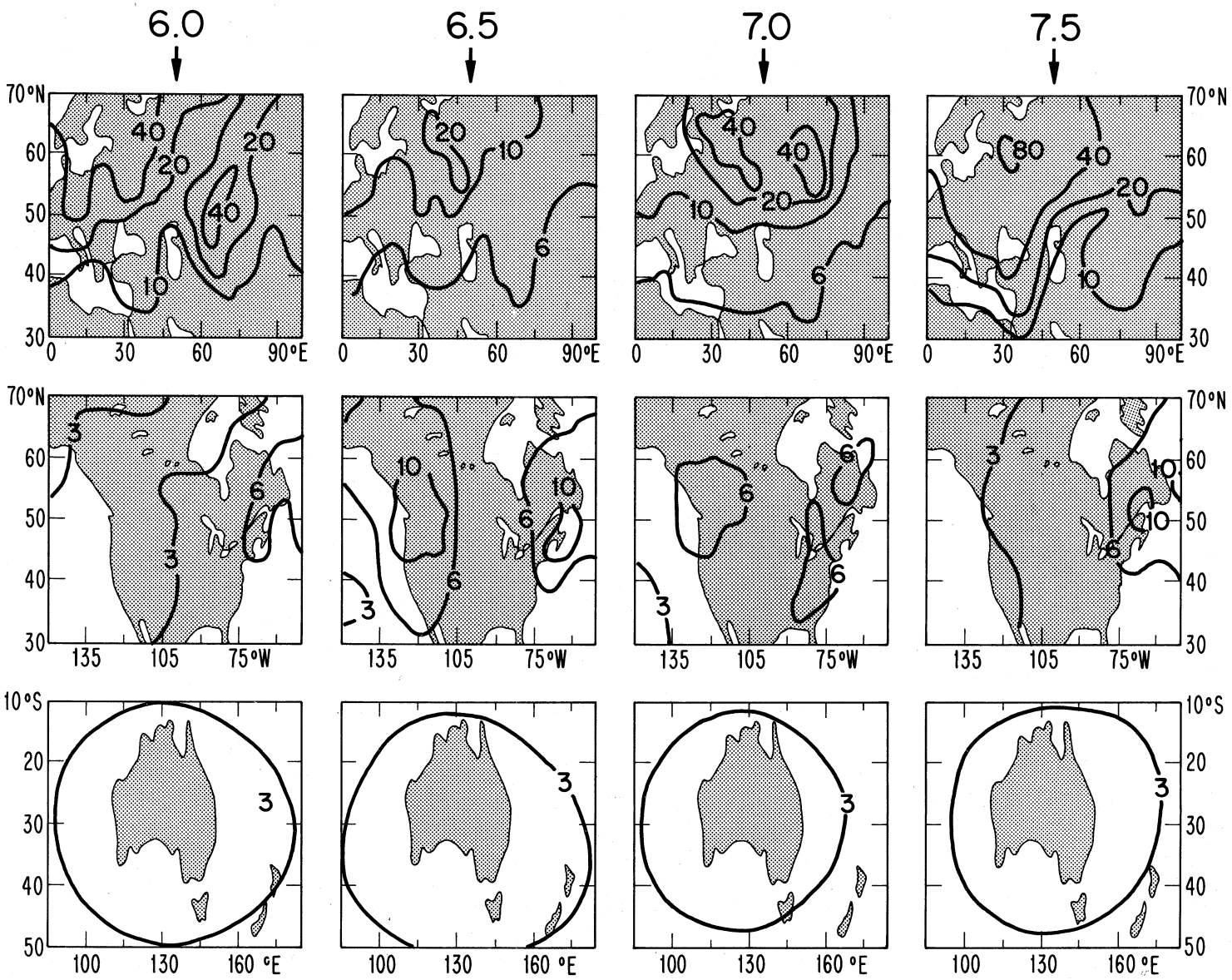

Figure 15. Behavior of the HF radio environment at local dusk above Eurasia, North America, and Australia for frequencies of 6.0, 6.5, 7.0, and 7.5 MHz during the period September-November 1977. Contours are receiver output voltage (millivolts × 10^{-2}).

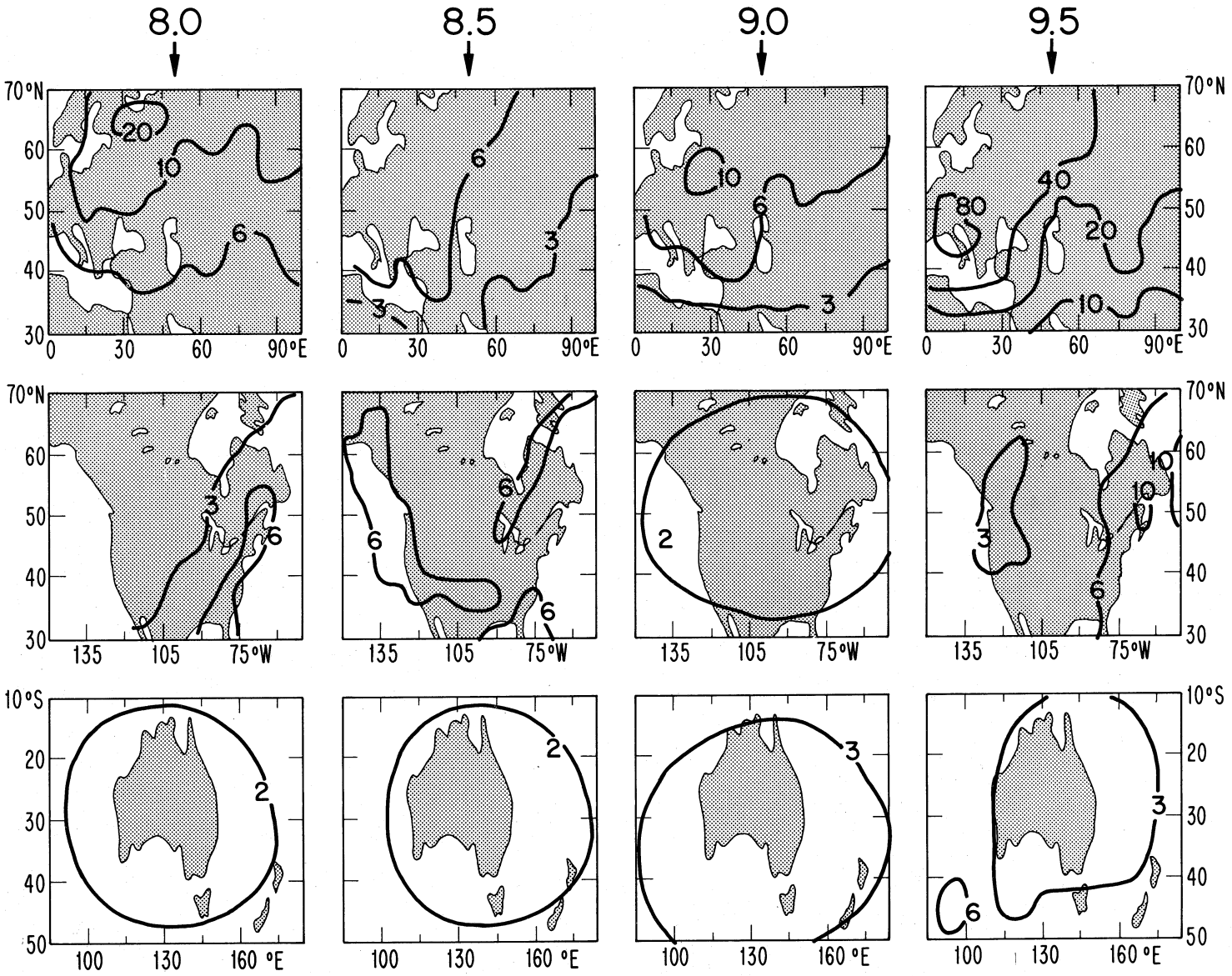

Figure 16. Behavior of the HF radio environment at local dusk above Eurasia, North America, and Australia for frequencies of 8.0, 8.5, 9.0, and 9.5 MHz during the period September-November 1977. Contours are receiver output voltage (millivolts $\times 10^{-2}$).

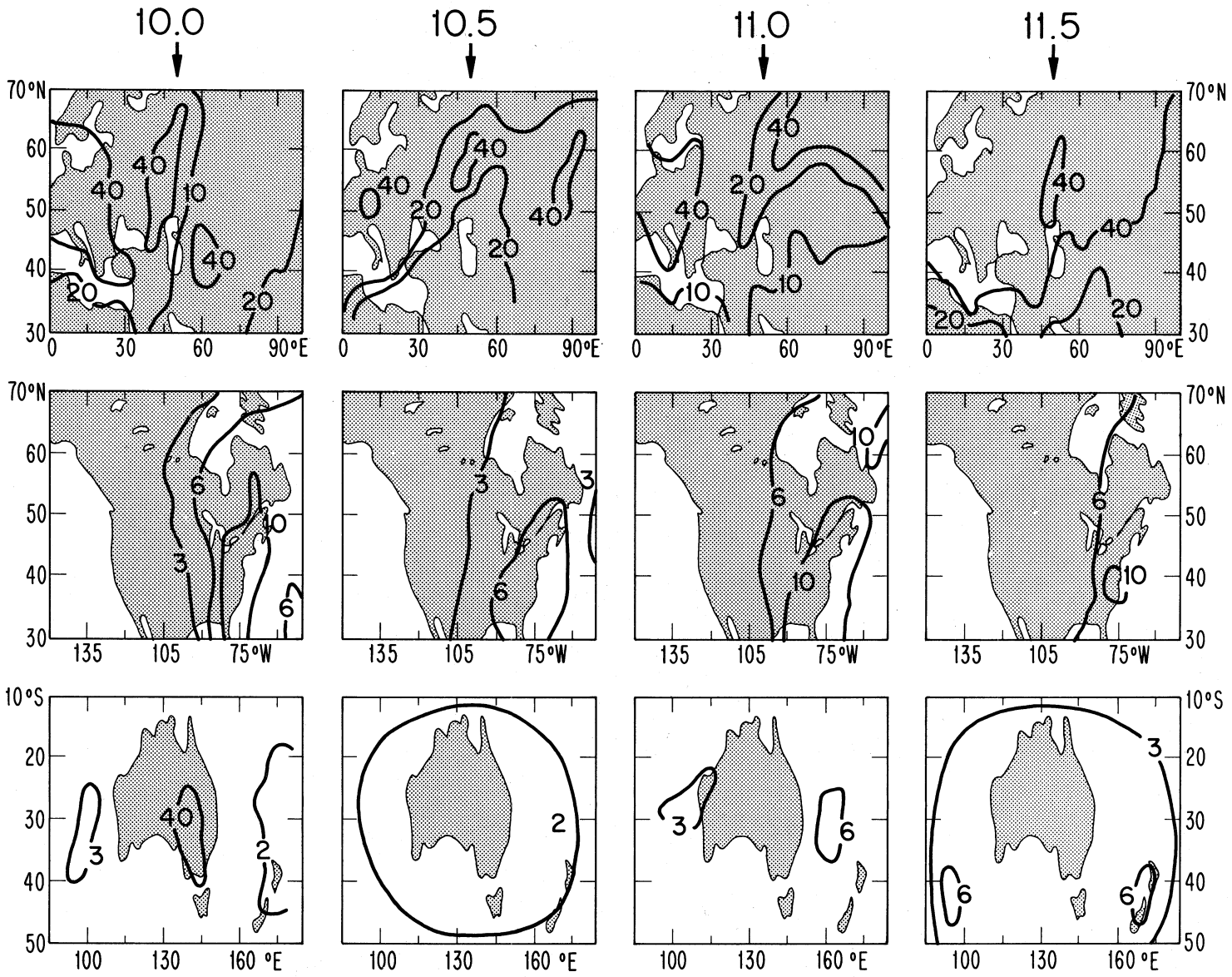

Figure 17. Behavior of the HF radio environment at local dusk above Eurasia, North America, and Australia for frequencies of 10.0, 10.5, 11.0, and 11.5 MHz during the period September-November 1977. Contours are receiver output voltage (millivolts × 10^{-2}).

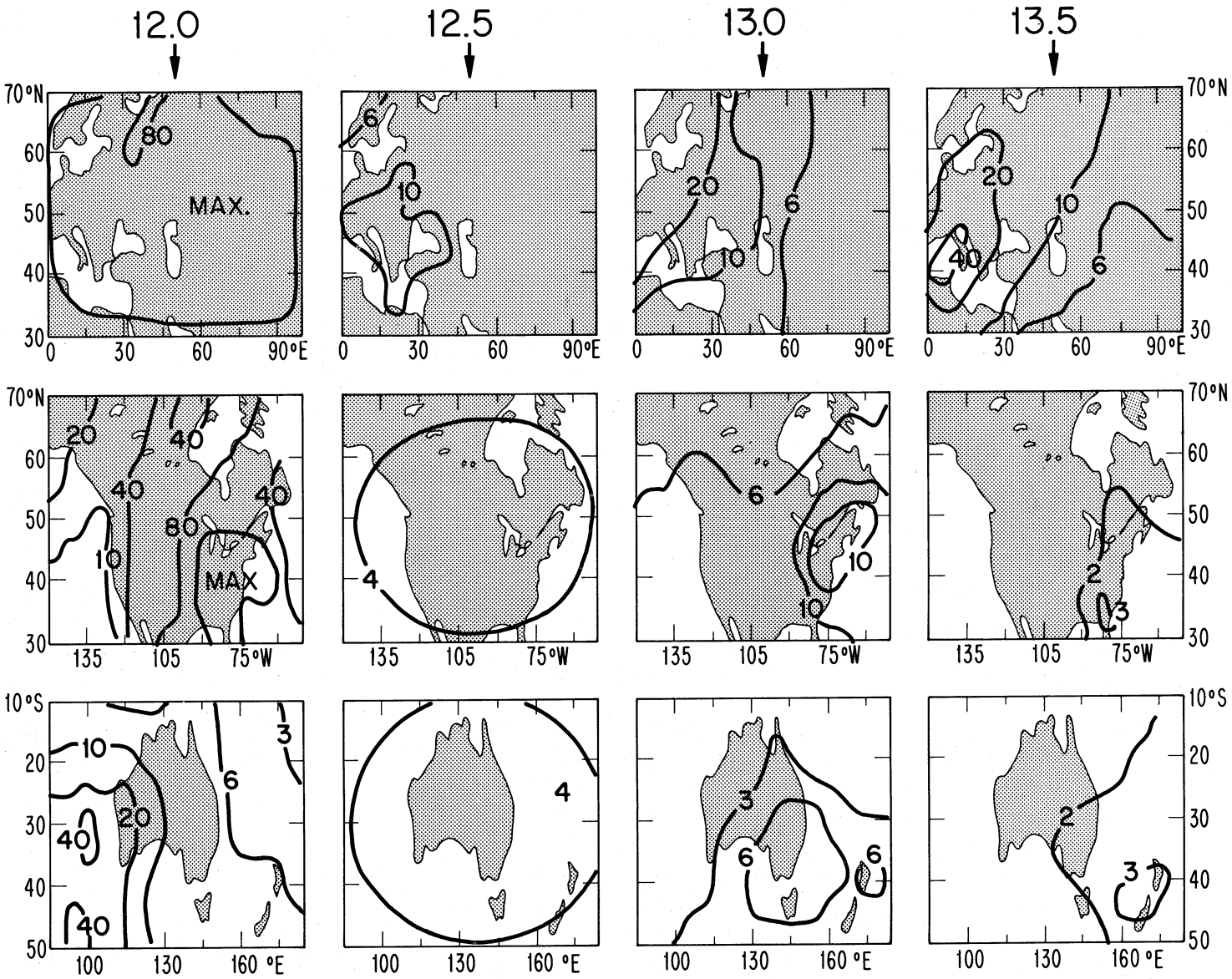

Figure 18. Behavior of the HF radio environment at local dusk above Eurasia, North America, and Australia for frequencies 12.0, 12.5, 13.0, and 13.5 MHz during the period September-November 1977. Contours are receiver output voltage (millivolts × 10^{-2}).

Figures 9 through 13 and 14 through 18 provide an indication of how the HF radio environment appears above different regions of the globe as well as how it varies with frequency at local dawn and dusk. The region of highest noise intensity consistently appears to be Eurasia with minor exceptions (for example, at 13.0 MHz during dawn and dusk), and the region showing the least amount of activity always tends to occur above Australia. The Eurasian area shows significant differences in the intensity of the HF radio environment even within the area itself, with "hot-spots" appearing at more than one location for a number of different frequencies. The results for the North American sector tend to display "hot-spots" that are aligned along the east and west coasts of the United States for a number of frequencies, particularly at 6.5, 9.5, 12.0, and 13.0 MHz. Substantial values of HF noise are seen to occur above Australia only at 12.0, 13.0, and somewhat at 13.5 MHz. The figures display the fact that there is little difference between the results obtained during local dawn and during local dusk. The most intense noise observations are seen for the frequencies of 6.0, 9.5, and 12.0 MHz. The smallest intensities tend to occur at frequencies of 8.5, 12.5, 13.0, and 13.5 MHz. There is no evidence that the intensity of the noise increases as the frequency increases, which would be the case if the earth were covered with noise sources distributed uniformly in frequency and location.

5.4. Studies of a Localized Effect

In generating the maps that were used to derive Figures 9 through 18, the appearance of an apparent source of noise to the west of Australia at the frequency of 11.5 MHz was noted during the dusk period. This apparent source of noise appeared to vary in intensity throughout the course of the time period September through November 1977. Figure 19 shows the behavior of the 11.5 MHz signal strength for a 12-day period in November 1977. It is readily apparent that the source is active on 14 November, reaches its maximum intensity on 15 November, and tends to disappear by 20 November, 1977. The cause of this source of noise and its variation with time is still under study.

5.5. Studies of Seasonal Effects

It is well-known that the ionosphere displays significant variations in its structure with regard to season. It is worthwhile investigating the degree to which the results described in the previous sections are dependent upon season. Figure 20a and 20b, 21a and 21b, and 22a and 22b illustrate global maps of the HF radio environment averaged over 10 days in April 1978 for the frequencies of 11.8, 8.5,

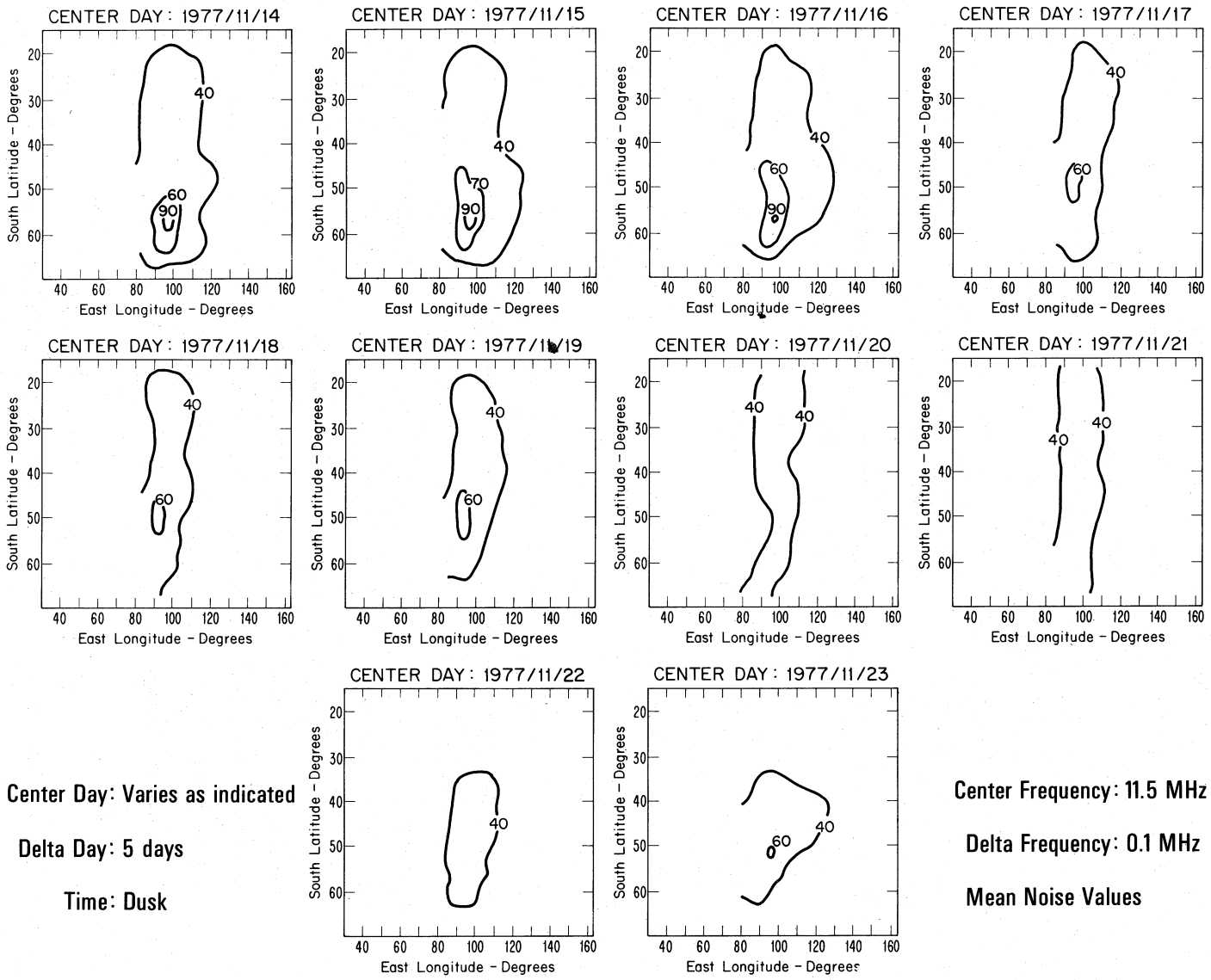

Figure 19. Contours of the receiver output voltage observed at 11.5 MHz during the times indicated. Contours are given in millivolts $\times 10^{-3}$.

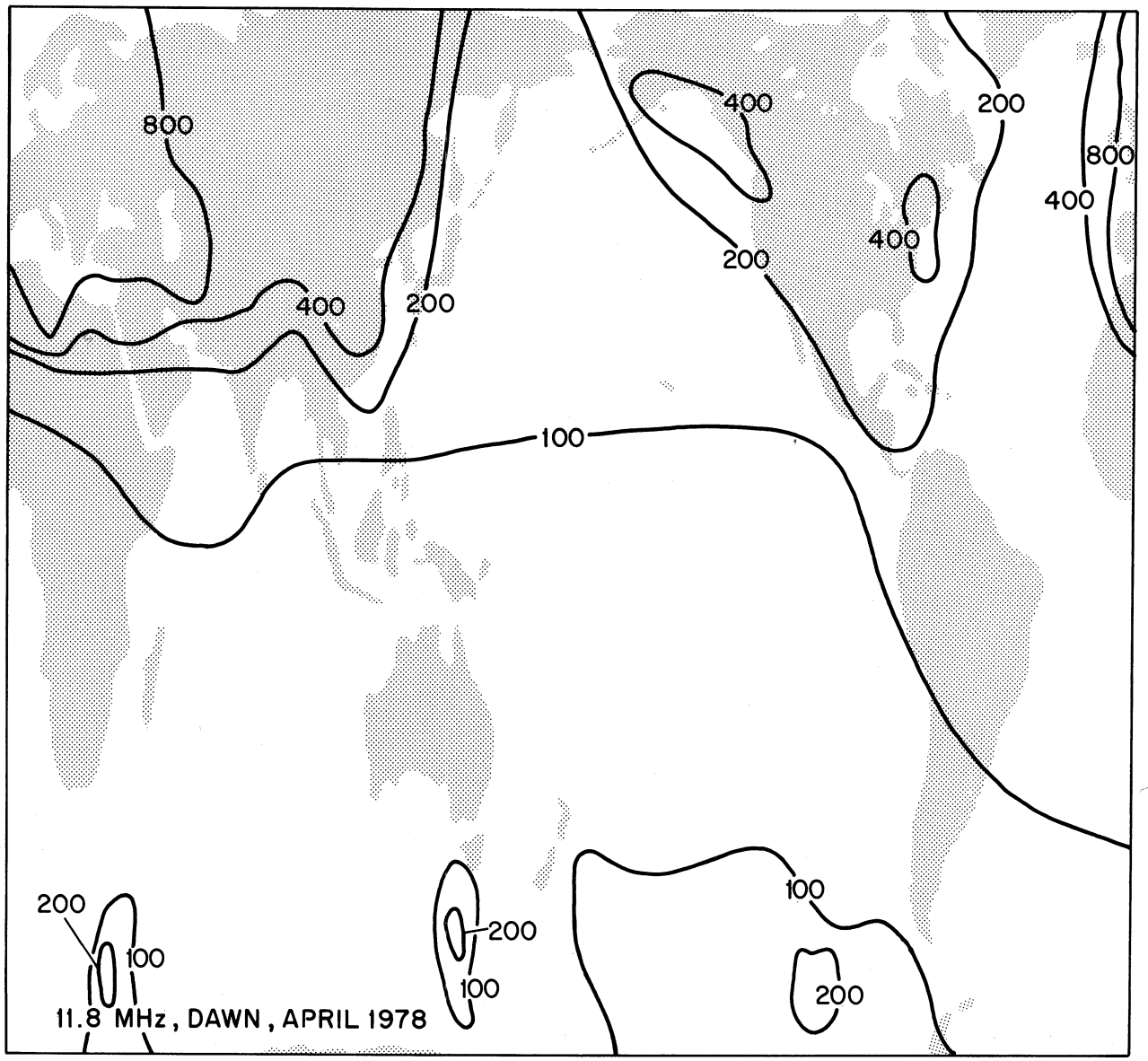

Figure 20a. Global distribution of radio noise observed at 11.8 MHz during the dawn period of April 1978. Contours are receiver output voltage (millivolts $\times 10^{-3}$).

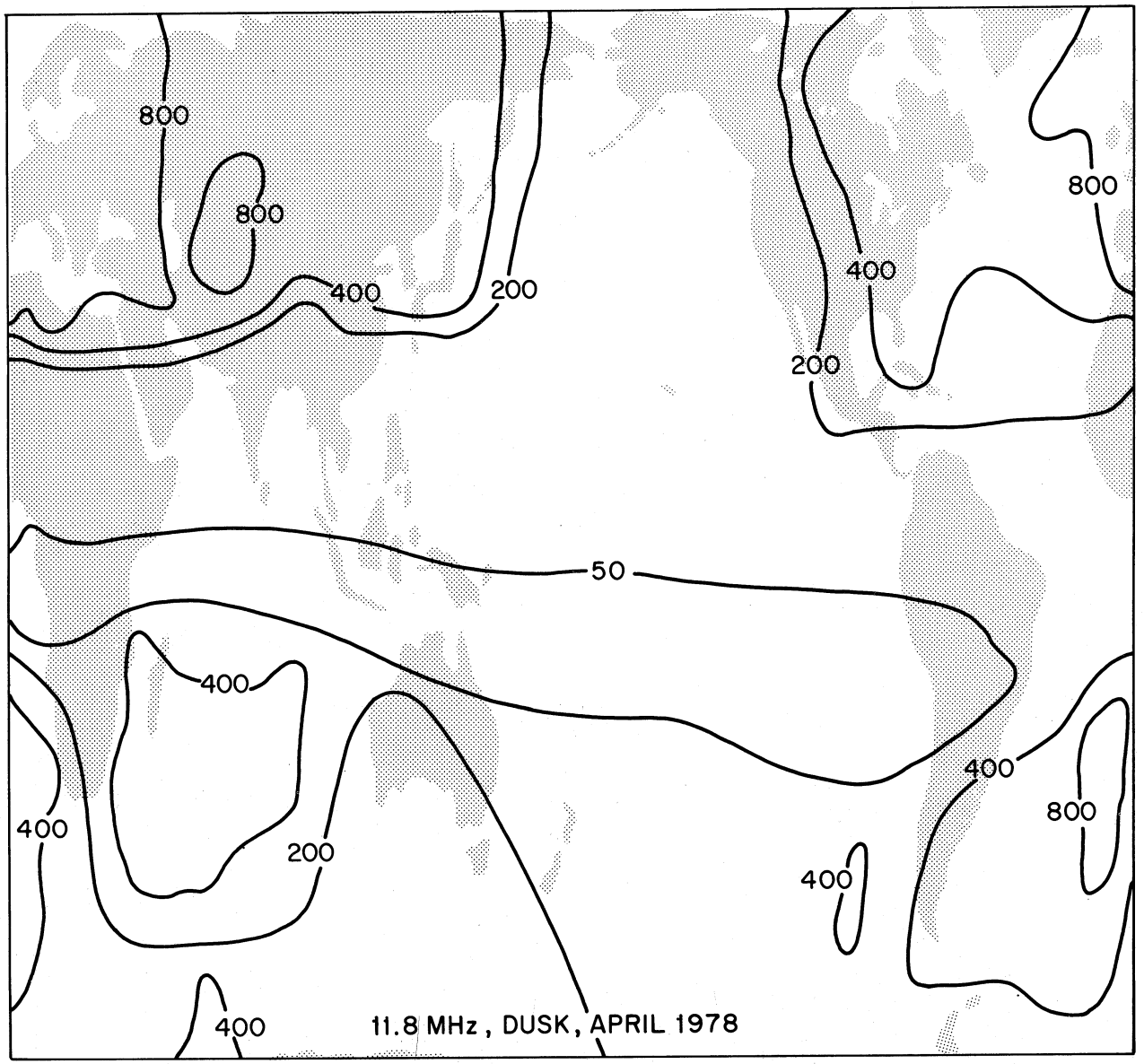

Figure 20b. Global distribution of radio noise observed at 11.8 MHz during the dusk period of April 1978. Contours are receiver output voltage (millivolts × 10^{-3}).

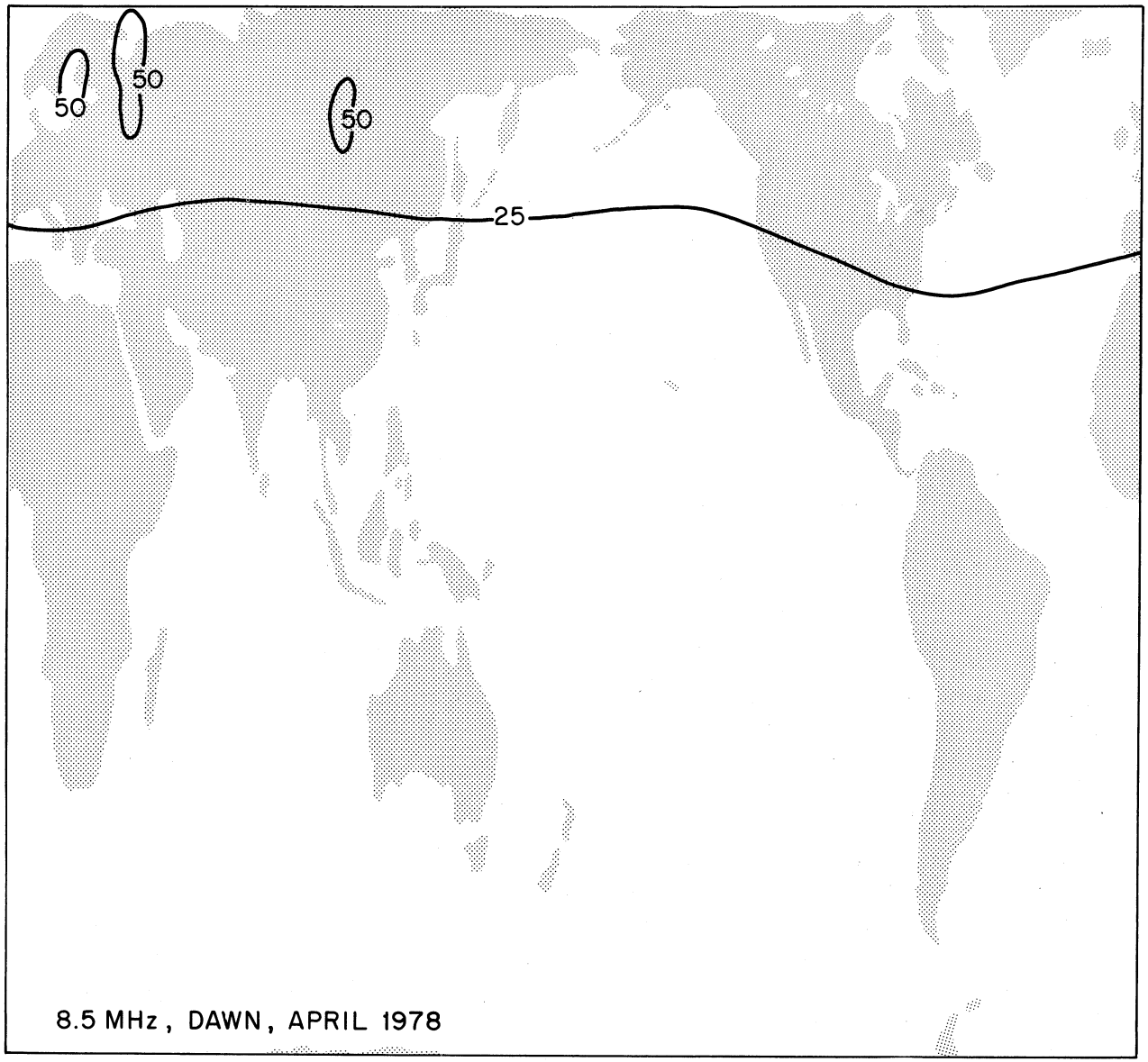

Figure 21a. Global distribution of radio noise observed at 8.5 Mhz during the dawn period of April 1978. Contours are receiver output voltage (millivolts $\times 10^{-3}$).

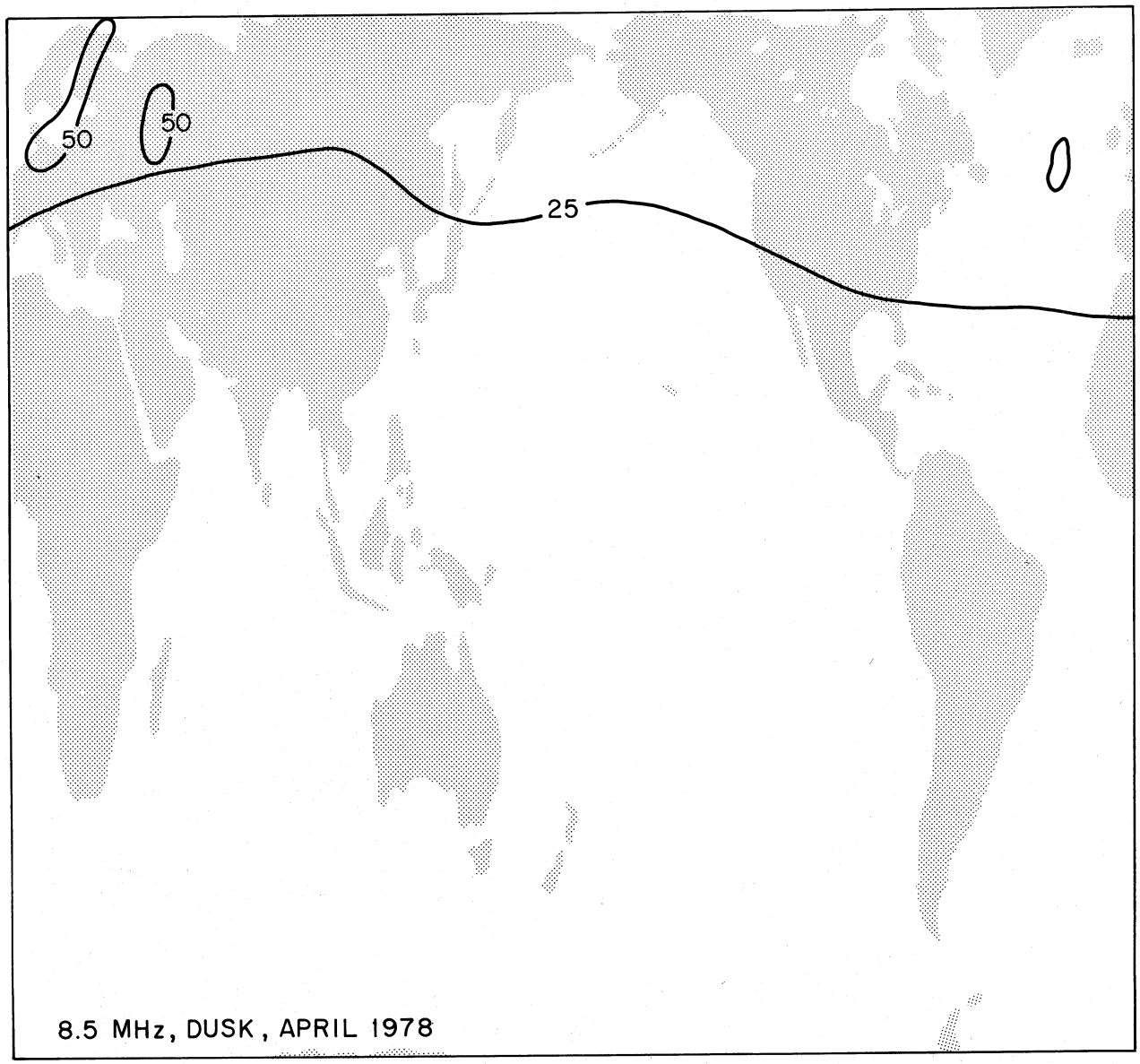

Figure 21b. Global distribution of radio noise observed at 8.5 MHz during the dusk period of April 1978. Contours are receiver output voltage (millivolts $\times 10^{-3}$).

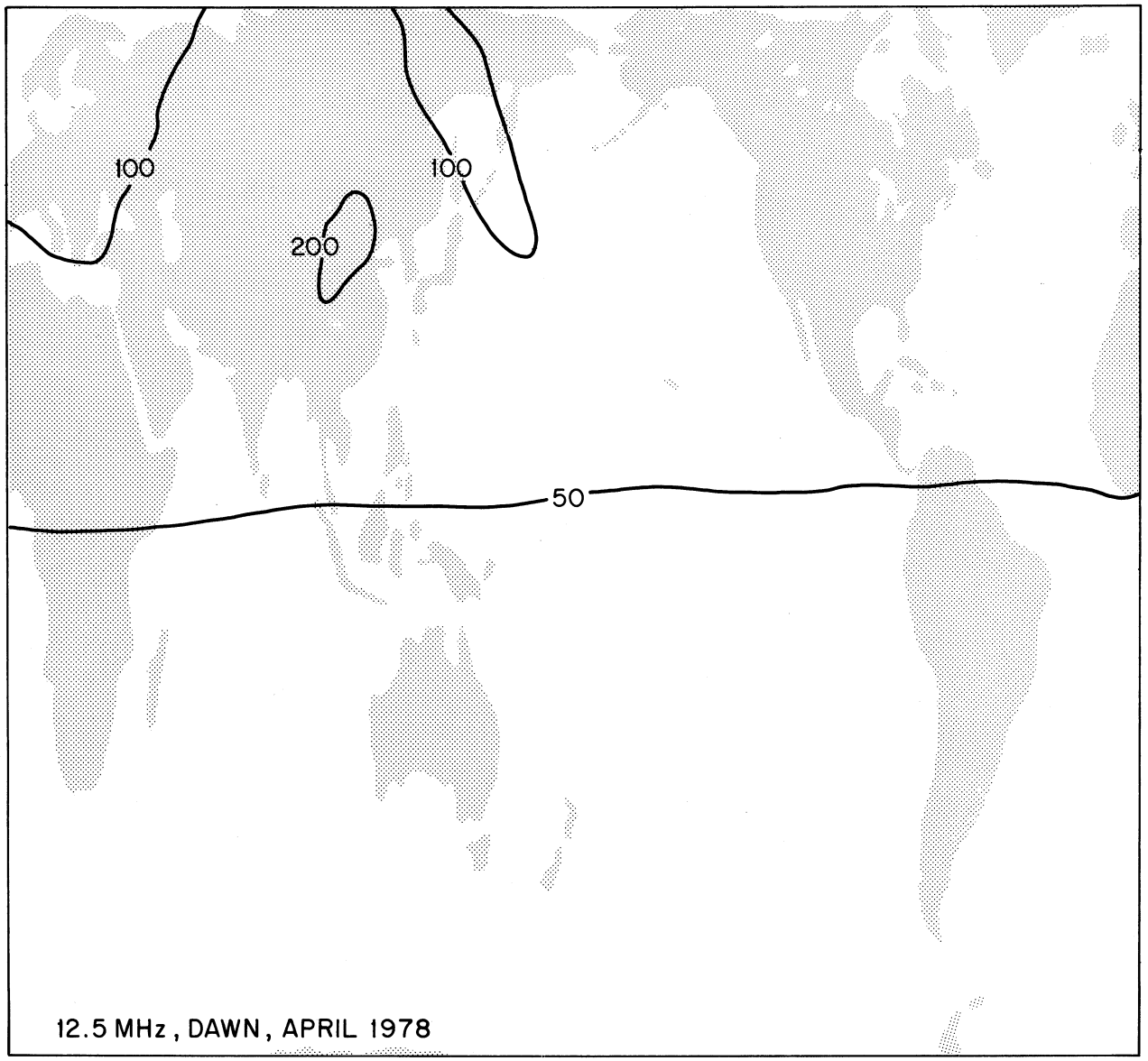

Figure 22a. Global distribution of radio noise observed at 12.5 MHz during the dawn period of April 1978. Contours are receiver output voltage (millivolts $\times 10^{-3}$).

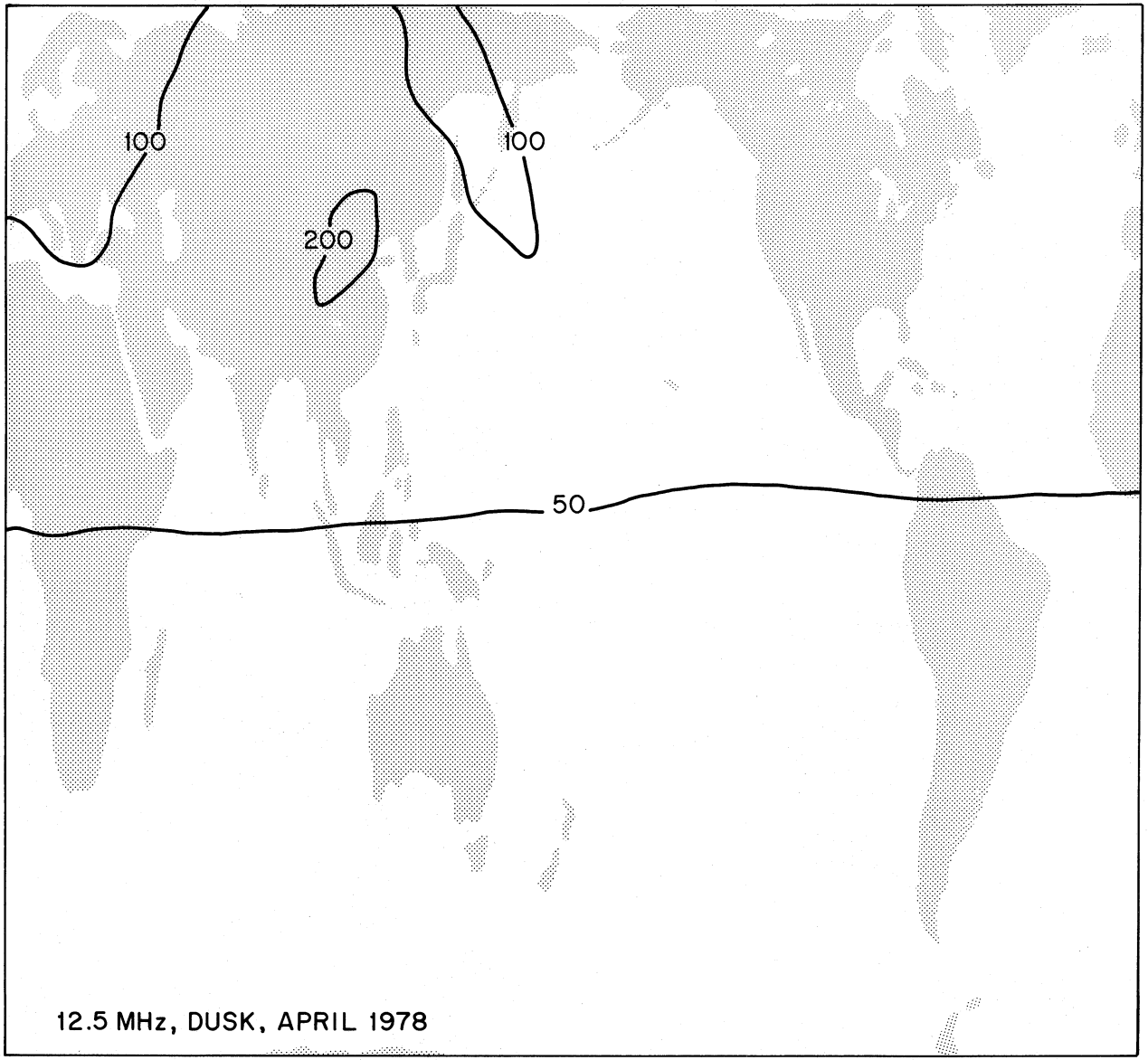

Figure 22b. Global distribution of radio noise observed at 12.5 MHz during the dusk period of April 1978. Contours are receiver output voltage (millivolts × 10^{-3}).

and 12.5 MHz. The maps are drawn for both the dawn and dusk periods, and the frequencies shown correspond exactly to those given in Figures 4, 7, and 8. It can be seen that the general features observed during the November time period are present during April viz: the frequency showing the highest magnitude of noise is 11.8 MHz, the global variations at 11.8 MHz are comparable during November and April (Figures 4 and 20), as are those for 8.5 MHz (Figures 7 and 21) and 12.5 MHz (Figures 8 and 22). There is a trend for the magnitudes of the 8.5 and 12.5 MHz results to be somewhat less in April compared to November, but the same geographical behavior persists in April and November.

Thus there appears evidence that there is little seasonal variation in the HF noise environment at the height of the DMSP satellite at least for dawn and dusk time periods. Clearly changes between frequencies are much more significant than changes for the same frequency as a function of season.

6. COMPARISON OF DATA WITH HF ALLOCATIONS

It is rather clear from the results shown in Figures 3 through 22 that the HF radio environment varies markedly as a function of frequency and as a function of location around the globe. If the sources of HF noise on the surface of the earth were distributed uniformly in frequency and in location, simple HF propagation theory indicates that, as the frequency increases, the noise observed by the satellite should increase. This is not the case observed by the HF receiver on-board the DMSP satellite, however. There is clear evidence that the intensity of the HF radio environment at a lower frequency can greatly exceed that of a higher frequency (12.0 MHz compared to 13.0 MHz, for example). The results also show that the highest observed intensities in the topside ionosphere occur above land areas of the globe and that not all of the land areas display comparable results. This is particularly the case when comparing Northern Hemisphere results with those obtained above the Southern Hemisphere. The noise intensity at any point in the topside ionosphere is dependent upon the characteristics of the sources of HF radio energy that are distributed over the globe as well as the characteristics of the intervening ionosphere.

The HF radio environment at satellite heights is a composite environment that results from the reception of all HF energy propagated to the satellite. The sources of this energy can be terrestrial lightning (atmospheric noise), unintentional man-made noise (due to industrial activity), and discretely radiated electromagnetic transmissions, all of which are expected to attain varying degrees of importance at varying times and locations. Obviously, if the sources of the noise reaching the

satellite are manmade, such as that due to industrial activity or discrete HF transmissions, the sources should, on the average, appear to be congregated over land areas.

The absence of any obvious atmospheric noise sources in the tropical regions seems to indicate that atmospheric noise is not contributing in a substantial manner to the observations presented here. It is possible that the receiver on the DMSP satellite operates in such a fashion as to discriminate against atmospheric noise. The receiver dwells at a given frequency for 250 milliseconds, during which time it integrates the signals that are received at the satellite. This integration process could minimize the amplitudes of the atmospheric noise since lightning-caused noise is rather impulsive in nature. The resulting spectrum would show a relative absence of atmospheric noise enhancements.

The intensity of the signals due to industrial activity varies over the globe according to the level of industrial sophistication. At the frequencies of interest in this study, the primary source of manmade industrial signals can be taken to be radiation from power lines which are substantially smaller than the signals associated with terrestrial transmitters. Obviously, it is rather difficult to obtain a detailed specification of the intensity of the total emissions in a given bandwidth at a given frequency. Estimates can be obtained by consulting the international frequency lists recorded by the International Frequency Registration Board (IFRB). These lists, however, are compilations of requests for frequency authorization that have been approved by the IFRB, and they can only be used as very rough estimates of the general properties of the HF spectrum utilization.

If the primary source of the noise observed by the DMSP satellite is in fact due to discrete transmissions, then the satellite HF noise observations must follow the manner in which the electromagnetic spectrum in the HF bands is allocated, at least in general terms. In Table 2, we have listed the classes of radio services that have been allocated by agreement under the International Telecommunications Union (ITU) for operation within $\pm$100 kHz of the frequency listed (100 kHz being chosen since it is the bandwidth of the DMSP receiver). We have also indicated how the spectrum allocation varies with Telecommunications Region (Europe falls in Region 1, Australia in Region 2, and North America in Region 3).

If the arguments presented above are in general correct, then, based on Table 2, the frequencies of 4.0, 5.0, 6.0, 9.5, and 12.0 MHz, being representative of frequencies allocated to the Broadcasting Service, should show the highest noise levels. Referring to Figures 4 through 22, it is readily apparent that the frequencies of 9.5, 9.6, 11.8, and 12.0 MHz do, in fact, display the highest noise levels

Table 2: Classes of Radio Services Allocated Within ±100 kHz of the Frequency Indicated

FREQUENCY	TELECOMMUNICATION REGION		
	REGION 1	REGION 2	REGION 3
4.0	AM;F;B	AM;F;MM	AM;B;F;MM
4.5	F;M		
5.0	F;LM;B;SF		
5.5	F;AM;LM	AM	F;M;LM
6.0	B;F		
6.5	AM;MM		
7.0	F;Am		
7.5	FIXED		
8.0	FIXED		
8.5	MARITIME MOBILE		
9.0	F;AM		
9.5	B;F		
10.0	F;AM;SF		
10.5	FIXED		
11.0	FIXED		
11.5	FIXED		
12.0	B;F		
12.5	MARITIME MOBILE		
13.0	MARITIME MOBILE		
13.5	FIXED		

KEY:
AM - Aeronautical Mobile
LM - Land Mobile
MM - Maritime Mobile
M - Mobile
F - Fixed
B - Broadcasting
Am - Amateur
SF - Standard Frequency

for each of the three regions of the earth shown. Above Europe, the frequency of 6.0 MHz also shows very high noise levels.

The results of other frequencies display similar types of agreement between observation and expectation based on Table 2. The frequencies of 6.5, 8.5, and 13.0 MHz, for example, are allocated to the Maritime Mobile Service. It is clear that, above North America, the contours at all three frequencies appear to be centered at the edges of large bodies of water as would be expected from transmissions in the Maritime Mobile Service. Above Europe, which shows the most activity in general, there is clear evidence that the frequencies above 6.0 MHz allocated to the maritime and aeronautical mobile services (6.5, 8.5, 12.5, and 13.0 MHz) do not show values of noise intensity as high as those allocated to the fixed services (7.0, 7.5, 8.0, 9.0, 10.0, 10.5, 11.0, and 11.5 MHz). Since fixed service transmissions tend to be more powerful than those of the maritime or aeronautical mobile services, this observation is in concert with the manner in which the HF spectrum is used by operators of discrete transmission systems.

It is apparent that, within the limits of uncertainty concerning the actual utilization of the HF spectrum (operational schedules, locations of transmitters, antenna radiation patterns, and the radiated power of on-air transmitters), the receiver on-board the DMSP satellite is sensitive to discrete manmade transmissions. The results indicate that the general behavior of the observed HF environment at the height of the satellite is in agreement with the manner in which the HF spectrum is allocated. Although the contributions to the HF environment made by sources due to industrial activity and lightning discharges cannot be ruled out entirely, it is not very likely that these sources are contributing in a substantial manner to the structure observed by the DMSP satellite.

The fact that the DMSP results appear to agree with how the electromagnetic spectrum is allocated has impact upon the manner in which observations of radio noise are averaged over frequency bands. This averaging could result either from combining adjacent frequencies of DMSP observations or from analyzing data obtained from a very wide-band receiver (bandwidth >200 kHz). Results of averaging DMSP data over varying frequency bands showed that, as long as the averaging is performed over adjacent frequencies allocated to the same class of service, meaningful and consistent results were obtained. If the combining of adjacent frequencies was effected over bands allocated to different services, the ensuing results were somewhat confused. This is illustrated in Figures 23 and 24, which show contours of HF noise averaged over 100 kHz centered on 11.3 MHz (Figure 24) and averaged over 1.2 MHz centered on the same 11.3 MHz (Figure 24). The data used to develop Figure 23

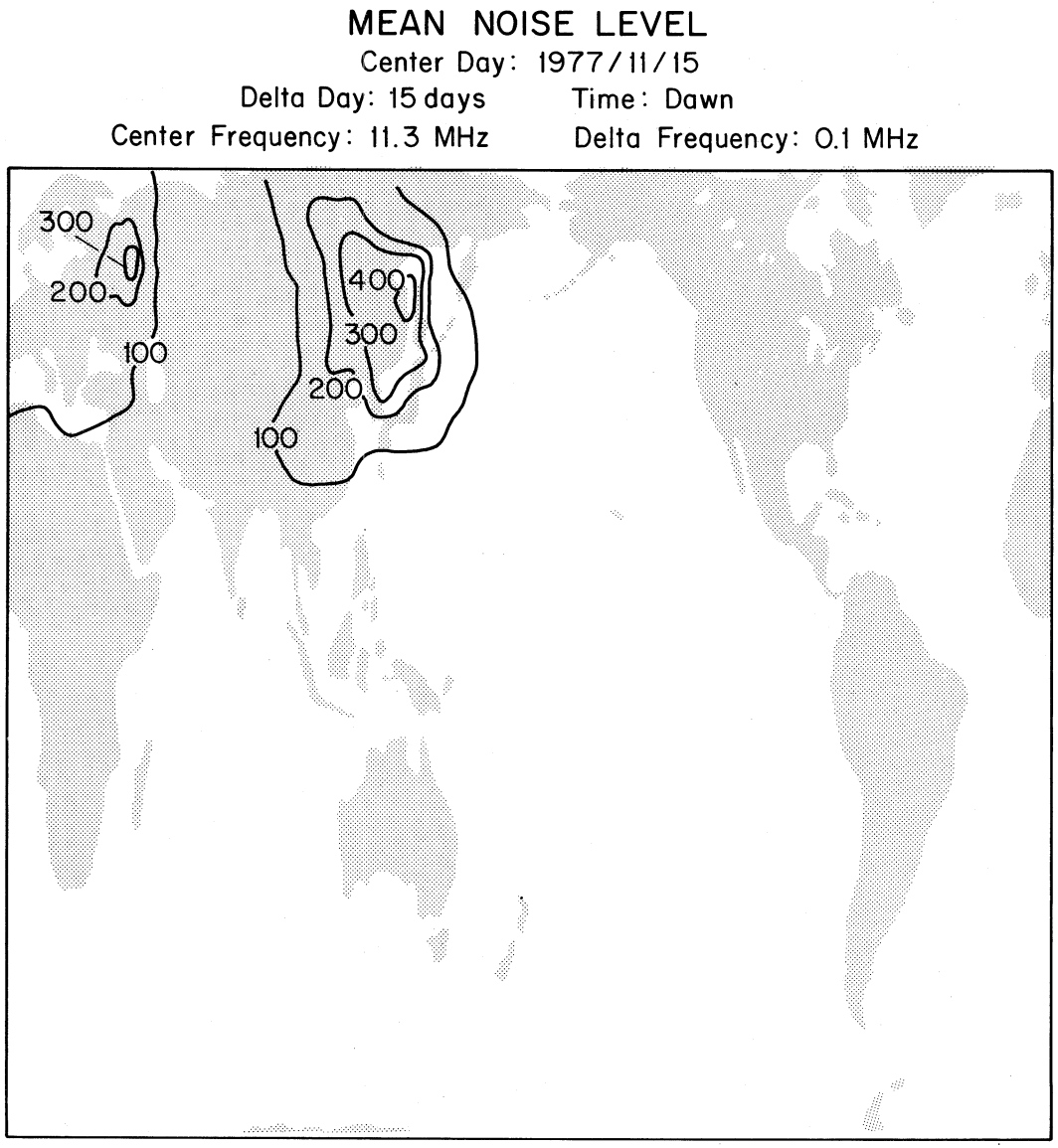

Figure 23. Global distribution of radio noise observed at 11.3 MHz during the dawn period of November 1977 averaged over 100 KHz. Contours are given in receiver output voltage (millivolts $\times 10^{-3}$).

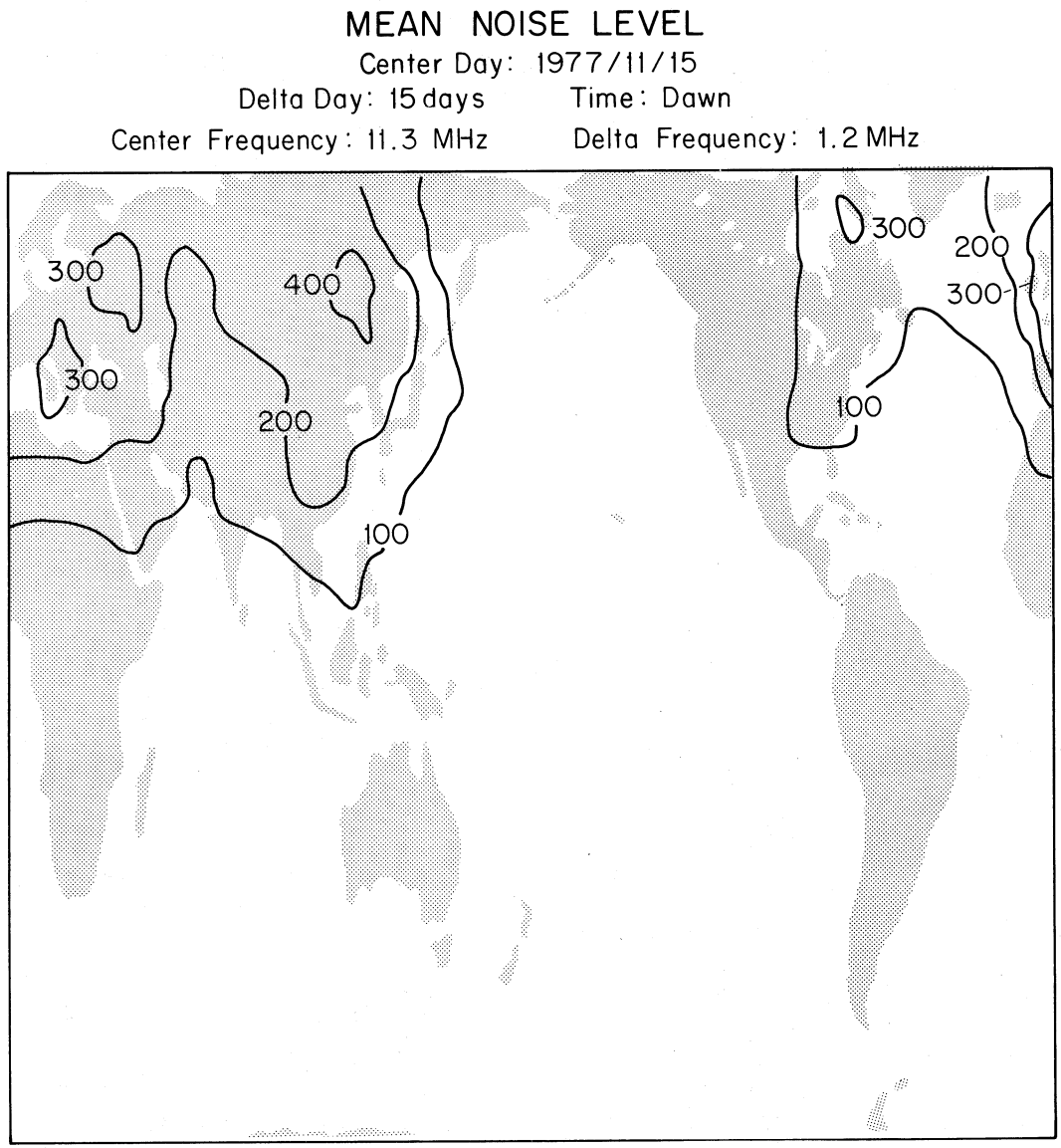

Figure 24. Global distribution of radio noise observed at 11.3 MHz during the dawn period of November 1977 averaged over 1.2 MHz. Contours are given in receiver output voltage (millivolts $\times 10^{-3}$).

pertain to a frequency interval that lies totally within the fixed service band. The data used to develop Figure 24 pertain to a frequency interval that combines the fixed service and broadcast service bands.

7. CONCLUSION

The results and discussion presented here indicate that the HF radio environment observed in the topside ionosphere by the Defense Meteorological Satellite (DMSP) is due primarily to discrete manmade transmissions. This conclusion is based on the fact that the results obtained appear to be in general agreement with the manner in which the HF spectrum is allocated and used. The most intense noise levels occur for those frequencies corresponding to allocations to the long-distance broadcasting service. The relative locations of the noise contours for frequencies allocated to the Maritime and Aeronautical Mobile Services add further weight to this conclusion. It is not possible to know exactly the detailed operational schedule of all electromagnetic transmission systems; thus, the general agreement between the DMSP results and spectrum allocation is taken as a convincing argument as to the sources of the DMSP noise levels.

The results show that the frequencies allocated to the long-distance broadcasting service have the highest levels, followed by those allocated to the fixed service. It is interesting to speculate whether this feature will persist throughout all hours of the day and also whether the European-Asian area would continue to show the most intense noise levels. The fact that the Eurasian area displays the greatest extent of the highest noise levels for frequencies in the Broadcast Service is also in agreement with general concepts of spectrum utilization. During local dawn in the Eurasian area, the local time in North America is in the evening hours, which coincidentally corresponds to the prime transmitting hours of broadcasts to North America from Europe. Similarly, it is anticipated that, during hours surrounding local dusk, European broadcasts would be directed toward Africa and the Middle East, thereby showing large values of HF noise in the DMSP results.

The results of this study also show that data averaged over a 10-15-day consecutive period are needed in order to develop realistic global maps of HF radio noise in the topside ionosphere. When averaging over adjacent frequencies, care should be taken to assure that the frequencies are allocated to the same class of service.

Further studies are needed to calibrate the HF receivers operating on the DMSP satellites. A program to undertake this calibration using a known terrestrial transmitter--the Platteville Ionospheric Heating Facility--is being planned for the near future. A recent DMSP satellite was launched into a noon-midnight orbit and

it too contained an HF receiver. Data taken from both the dawn-dusk and noon-midnight satellites should be analyzed for the same time periods to study how the HF radio environment in the topside ionosphere varies as a function of time of day and of season.

8. REFERENCES

Alexander, J. K., L. W. Brown, T. A. Clark, R. G. Stoner, and R. R. Webber (1969a), The spectrum of the cosmic radio background between 0.4 and 6.5 MHz, Astrophys. J. 157, p. L163.

Alexander, J. K., H. H. Malitson, and R. G. Stone (1969b), Type III radio bursts in the outer corona, Solar Phys., 8, p. 388.

CCIR, International Radio Consultative Committee (1963), Report 322, World distribution and character of atmospheric noise, Documents of the Xth Plenary Assembly, Geneva.

CCIR, International Radio Consultative Committee (1978), Report 340-3, CCIR atlas of ionospheric characteristics, Documents of the XIVth Plenary Assembly, Kyoto.

Crichlow, W. Z., R. C. Davis, R. T. Disney, and M. W. Clark (April 1971), Hourly probability of world-wide thunderstorm occurrence, Telecommunications Research Report, OT/ITS RR 12, Boulder, CO.

Gurnett, D. A. (1975), The earth as a radio source: The non-thermal continuum, J. Geophys. Res., 80, pp. 2751-2763.

Hakura, Y., R. Nishizaki, K. Tao, and F. Yamashita (1970), Observation of solar radio bursts by the satellite Alouette II during the PFP interval, May-July 1969, J. Radio Res. Labs., Japan, 17, p. 21.

Hartz, T. R. (1964a), Observations of the galactic radio emission between 1.5 and 10 Mc/s from the Alouette satellite, Ann. Astrophys., 27, p. 823.

Hartz, T. R. (1964b), Solar noise observations from the Alouette satellite, Ann. Astrophys., 27, p. 831.

Hartz, T. R. (1969), Radio noise levels within and above the ionosphere, Proc. IEEE, 57, pp. 1042-1050.

Herman, J. R., J. A. Caruso, and R. G. Stone (1973), Radio astronomy exployer RAG-1 observations of terrestrial radio noise, Planet. Space Sci., 21, pp. 443-461.

Herman, J. R., R. G. Stone, and J. A. Caruso (1975), Radio detection of thunderstorm activity with an earth-orbiting satellite, J. Geophys. Res., 80, pp. 665-672.

Horner, F., and R. B. Bent (1969), Measurement of terrestrial radio noise, Proc. Roy. Soc. A, 311, pp. 525-542.

Kurth, W. S., M. M. Baumback, and D. A. Gurnett (1975), Direction-finding measurements of auroral kilometric radiation, J. Geophys. Res., 80, pp. 665-672.

Maliphant, R. G. (1967), Ionospheric refraction of high-frequency radio wave propagating between the earth and orbiting satellites, Propagation factors in space communications, AGARD Conf. Proc., 3 (edited by W. T. Blackband), 85, Technivision, Maidenhead, England.

Rush, C. M. and J. Buchau (1977), Determining the F-region critical frequency from satellite-borne noise measurements, J. Atmos. Terr. Phys., 39, pp. 277-286.

Rush, C. M. and E. Ziemba (1978), On the usefulness of topside HF noise measurements in determining foF2, J. Atmos. Terr. Phys., 40, pp. 1073-1079.

Rush, C. M., D. Nelson, A. L. Snyder, V. Patterson, T. Tascione, and E. Ziemba (January 24-26, 1978), HF noise-space, Proc. of 1978 Sym. on Effects of the Ionosphere on Space and Terrestrial Systems, Washington, D. C.

Walsh, D., F. T. Haddock (1964), Cosmic radio intensities at 1-225 and 2-0 Mc/s measured up to an altitude of 1700 km., Space Research IV (Ed. P. Muller), North-Holland Publ. Co., Amsterdam, p. 935.

FORM OT-29
(3-73)

U.S. DEPARTMENT OF COMMERCE
OFFICE OF TELECOMMUNICATIONS

BIBLIOGRAPHIC DATA SHEET

	1. PUBLICATION OR REPORT NO. NTIA Report 80-33	2. Gov't Accession No.
3. Recipient's Accession No.		
4. TITLE AND SUBTITLE HF Radio Noise in the Topside Ionosphere		5. Publication Date February 1980
		6. Performing Organization Code
7. AUTHOR(S) Charles M. Rush, Rayner K. Rosich, & Carlene Mellecker		9. Project/Task/Work Unit No. 910 3565
8. PERFORMING ORGANIZATION NAME AND ADDRESS National Telecommunications & Information Administration Institute for Telecommunication Sciences 3413-1 325 Broadway Boulder, CO 80303		10. Contract/Grant No.
11. Sponsoring Organization Name and Address AFGL Hanscom AFB, MA 01731		12. Type of Report and Period Covered
		13.

14. SUPPLEMENTARY NOTES

15. ABSTRACT *(A 200-word or less factual summary of most significant information. If document includes a significant bibliography or literature survey, mention it here.)*

Radio noise of ground-based origin can be observed by a satellite-borne receiver orbiting above the F2 region. The noise that is observed is a function of receiver frequency, satellite position, and local time at the sub-satellite point. A recently launched Defense Meteorological Satellite is equipped with a swept-frequency, high-frequency (HF) noise of terrestrial origin every 100 kHz in the frequency range 1.2 to 13.9 MHz. In this report, we discuss the characteristics of the noise environment as observed by the satellite during periods surrounding local dawn and local dusk.

16. Key words *(Alphabetical order, separated by semicolons)*

KEY WORDS: DMSP Satellite; HF Propagation; HF Radio Noise; Spectrum Utilization.

17. AVAILABILITY STATEMENT [X] UNLIMITED. [ ] FOR OFFICIAL DISTRIBUTION.	18. Security Class *(This report)* UNCLASSIFIED	20. Number of pages
	19. Security Class *(This page)* UNCLASSIFIED	21. Price:

☆U.S. GOVERNMENT PRINTING OFFICE: 1980-0-677-305/248